GLOBAL HEALTH 2022

The Eleventh International Conference on Global Health Challenges

ISBN: 978-1-61208-995-9

November 13 - 17, 2022

Valencia, Spain

GLOBAL HEALTH 2022 Editors

Les Sztandera, Thomas Jefferson University, USA

GLOBAL HEALTH 2022

Forward

The Eleventh International Conference on Global Health Challenges (GLOBAL HEALTH 2022), held between November 13 and November 17, 2022, took a global perspective on population health, from national to cross-country approaches, multiplatform technologies, from drug design to medicine accessibility, everything under mobile, ubiquitous, and personalized characteristics of new age population.

Recent advances in technology and computational science influenced a large spectrum of branches in approaching population health. Despite significant progresses, many challenges exist, including health informatics, cross-country platforms interoperability, system and laws harmonization, protection of health data, practical solutions, accessibility to health services, and many others. Along with technological progress, personalized medicine, ambient assistance and pervasive health complement patient needs. A combination of classical and information-driven approach is developing now, where diagnosis systems, data protection mechanisms, remote assistance and hospital-processes are converging.

The conference had the following tracks:

- Health and Wellness Informatics
- Challenges
- Alternative
- Global

We take here the opportunity to warmly thank all the members of the GLOBAL HEALTH 2022 technical program committee, as well as all the reviewers. The creation of such a high quality conference program would not have been possible without their involvement. We also kindly thank all the authors that dedicated much of their time and effort to contribute to GLOBAL HEALTH 2022. We truly believe that, thanks to all these efforts, the final conference program consisted of top quality contributions.

We also gratefully thank the members of the GLOBAL HEALTH 2022 organizing committee for their help in handling the logistics and for their work that made this professional meeting a success.

We hope that GLOBAL HEALTH 2022 was a successful international forum for the exchange of ideas and results between academia and industry and to promote further progress in the domain of global health. We hope that Valencia provided a pleasant environment during the conference and everyone saved some time to enjoy the charm of the city.

GLOBAL HEALTH 2022 Steering Committee

Matthieu-P. Schapranow, Hasso Plattner Institute für Digital Engineering gGmbH, Germany
Lorena Parra Boronat, Instituto Madrileño de Investigación y Desarrollo Rural, Agrario y Alimentario and Universitat Politecnica de Valencia, Spain
Ah-Choo Koo, Research Centre for Interactive Media Faculty of Creative Multimedia, Multimedia University, Malaysia
Evgeniy Krastev, Sofia University St. Kliment Ohridsky, Bulgaria
Ozgu Can, Ege University, Turkey
Monique Chyba, University of Hawaiʻi at Mānoa, USA

GLOBAL HEALTH 2022 Publicity Chair

Mar Parra, Universitat Politecnica de Valencia, Spain
Sandra Viciano Tudela, Universitat Politecnica de Valencia, Spain

GLOBAL HEALTH 2022

COMMITTEE

GLOBAL HEALTH 2022 Steering Committee

Matthieu-P. Schapranow, Hasso-Plattner-Institut für Digital Engineering gGmbH, Germany
Lorena Parra Boronat, Instituto Madrileño de Investigación y Desarrollo Rural, Agrario y Alimentario and Universitat Politecnica de Valencia, Spain
Ah-Choo Koo, Research Centre for Interactive Media, Faculty of Creative Multimedia, Multimedia University, Malaysia
Evgeniy Krastev, Sofia University St. Kliment Ohridsky, Bulgaria
Ozgu Can, Ege University, Turkey
Monique Chyba, University of Hawaiʻi at Mānoa, USA

GLOBAL HEALTH 2022 Publicity Chair

Mar Parra, Universitat Politecnica de Valencia, Spain
Sandra Viciano Tudela, Universitat Politecnica de Valencia, Spain

GLOBAL HEALTH 2022 Technical Program Committee

Mohamed Basel Almourad, Zayed University, Dubai, UAE
Kyota Aoki, Utsunomiya University, Japan
Marzieh Ayati, University of Texas Rio Grande Valley, USA
Samuel Bamgbose, Prairie View A&M University, USA
Panagiotis D. Bamidis, School of Medicine - Aristotle University of Thessaloniki, Greece
Oresti Banos, University of Granada, Spain
Valérie Barbier, Mater Research Institute, Australia
Vilmos Bilicki, University of Szeged, Hungary
Ozgu Can, Ege University, Turkey
Chih-Lin Chi, University of Minnesota, USA
Javier Civit, COBER S.L., Seville, Spain
Sandra Costanzo, University of Calabria, Italy
Steven A. Demurjian, The University of Connecticut, USA
Jitender Singh Deogun, University of Nebraska - Lincoln, USA
Ivan Evgeniev, Technical UniversityofSofia, Bulgaria
Azeema Fareed, COMSATS, Pakistan
Marta Fernandez, Official College of Nursing of Madrid, Spain
John Gialelis, University of Patras, Greece
Marie-Pierre Gleizes, IRIT, France
Alexandra González Aguña, University of Alcala, Spain
Adela Grando, Arizona State University | College of Health Solutions / Mayo Clinic, USA
David Greenhalgh, University of Strathclyde, Glasgow, UK
Vida Groznik, University of Primorska & University of Ljubljana, Slovenia
Liang Gu, Sangfor Technologies Inc., China
Teresa Guarda, Universidad Estatal Peninsula Santa Elena - UPSE / Universidad de las Fuerzas Armadas -

ESPE / ALGORITMI Research Centre | ESPE | UPSE, Ecuador
Albert Guvenis, Institute of Biomedical Engineering | Boğaziçi Ünivesity, Turkey
Ying-Feng Hsu, Osaka University, Japan
Yasmeen Ali Hussein, University of Alkafeel, Iraq
Yuankai Huo, Vanderbilt University, USA
Zina Ibrahim, King's College London, UK
Kamran Iqbal, University of Arkansas at Little Rock, USA
Anđela Jakšić Stojanović, Universit Donja Gorica, Montenegro
Ravi Janardan, University of Minnesota-Twin Cities, USA
Rui Jesus, NOVA LINCS | Instituto Superior de Engenharia de Lisboa (ISEL) - Instituto Politécnico de Lisboa (IPL), Portugal
Dimitrios G. Katehakis, Center for eHealth Applications and Services FORTH -Institute of Computer Science, Greece
Ah-Choo Koo, Digital Cities Research Institute | Multimedia University, Malaysia
Evgeniy Krastev, Sofia University St. Kliment Ohridsky, Bulgaria
Li-Hui Lee, National Taipei University of Nursing and Health Sciences, Taipei, Taiwan
Elie Lefeuvre, Université Paris-Saclay – CNRS, France
Lenka Lhotska, Czech Technical University in Prague, Czech Republic
Jinfeng Li, Imperial College, UK
Siru Liu, University of Utah, USA
Igor Ljubi, University College for Applied Computer Engineering - Zagreb, Croatia
Matthias Loebe, Miami Transplant Institute | University of Miami Miller School of Medicine | Jackson Health Systems, USA
Fenglong Ma, Pennsylvania State University, USA
Flora Malamateniou, University of Piraeus, Greece
Stefano Mariani, Politecnico di Milano, Italy
Dulani Meedeniya, University of Moratuwa, Sri Lanka
Sushil K. Meher, All India Institute of Medical Sciences, India
Zeleke Mekonnen, Jimma University, Ethiopia
António H.J. Moreira, 2Ai – School of Technology | IPCA, Barcelos, Portugal
Pascal Mossuz, Institute of Biology and Pathology CHU Grenoble Alpes / Institut for Advanced bioscience (IAB) / University Grenoble-Alpes, France
Brendan O'Flynn, Tyndall Microsystems | University College Cork, Ireland
Elaheh Pourabbas, National Research Council | Institute of Systems Analysis and Computer Science "Antonio Ruberti", Roma, Italy
G M Atiqur Rahaman, Khulna University, Bangladesh
Álvaro Rocha, University of Lisbon, Portugal
Carsten Röcker, FraunhoferIOSB-INA, Germany
Nancy Rodriguez, LIRMM | Université de Montpellier | CNRS, France
Magda Rosenmoller, IESE Business School, Barcelona, Spain
Nandan Sarkar, Thapar Institute of Engineering and Technology, India
Laura Sbaffi, University of Sheffield, UK
Matthieu-P. Schapranow, Hasso-Plattner-Institut für DigitalEngineering gGmbH, Germany
Toria Shaw Morawski, Healthcare Information and Management Systems Society (HIMSS), USA
Pietro Siciliano, Institute for Microelectronics and Microsystems (IMM-CNR), Lecce, Italy
Joaquim P. Silva, Polythecnic Institute of Cávado and Ave, Portugal
Lina F. Soualmia, Normandy University, France
Paulo Sousa Teixeira, Polythecnic Institute of Cávado and Ave, Portugal

Table of Contents

Investigation of the Application of MediaPipe to Gait Analysis

Yasutaka Uchida
Dept. of Life Science
Teikyo University of Science
Adachi-ku, Tokyo, Japan
e-mail:uchida@ntu.ac.jp

Tomoko Funayama
Dept. of Occupational therapy
Teikyo University of Science
Uenohara-shi, Yamanashi, Japan
e-mail:funayama@ntu.ac.jp

Yoshiaki Kogure
Professor Emeritus
Teikyo University of Science
Adachi-ku, Tokyo, Japan
e-mail:kogure@ntu.ac.jp

***Abstract*— The possibility of gait analyses using moving images was examined using the free software, MediaPipe. As a preliminary experiment for using this software in the rehabilitation field, we attempted a timed up-and-go test and confirmed that detailed ankle trajectories were obtained. In addition, considering the limitations of the camera installation during measurement, we examined the differences in camera position when capturing gait characteristics. As a result, the characteristics captured were almost similar, although some discrepancies were observed between the frontal image and data from the oblique direction. Detection of the ankle angle was possible. However, it is likely that the right ankle data will be calculated to be smaller, regardless of motion limitations, and a motion analysis using gait velocity will require the placement of objects for correction. If free software becomes available for motion analyses, it will be a turning point for the rapid spread of video analyses in the medical and healthcare fields, contributing to the collection of improved data through rehabilitation and daily health management.**

Keywords-gait analysis; MediaPipe; detection of ankle angle; health care.

I. INTRODUCTION

Health status is easily expressed during gait. In addition, functional impairment of the lower extremities can lead to serious accidents such as falls and tumbles. Falls and tumbling are common social problems. Among the lower limbs, the limited range of motion of the ankle joint can easily lead to stumbling and falling due to the inability to raise the toes. The measurement of lower limb function is useful in assisting the prevention of falls. Until now, medical and welfare professionals, such as rehabilitation and nursing care staff, have been responsible for providing support to prevent falls. In recent years, devices for measuring lower limb function have become widespread. However, the equipment used in rehabilitation medicine and sports requires detailed data and specialized knowledge of equipment operations. It is also difficult to make decisions related to health conditions in daily life [1]-[6].

Wearable devices are slowly being used in daily life. Simultaneously, they can provide information about a runner's running route and speed, as well as information about the body, such as the pulse rate. This information can be used as management records by connecting it to the Internet. Daily health-related data managed by servers can be very useful for elderly people. Internet of things (IoT) devices are developed in many aspects, however, practically, it is important to be able to accumulate daily health information even if the person is unaware of it. If an IoT device can measure ankle joint data, it can help prevent falls and stumbling. Previously, we measured the gait of dialysis patients, however, but the analysis required specialized knowledge of machine learning [7].

MediaPipe is free software from Google. Numerical data can be obtained using software related to faces that specializes in facial data and poses corresponding to the entire body. It is also possible to display Three-Dimensional (3D) skeletons from Two-Dimensional (2D) detection on the screen. The ability to see images of the skeleton as it is projected onto the physique is a point that is easily accepted in rehabilitation facilities [8].

This software provides 3D coordinates that increase its effectiveness. Specifically, if ankle angles could be obtained from images, it could be a promising alternative to the judgment of physical condition changes based on the experience of physical and occupational therapists. Long-term ankle angle data would also be useful for early detection of changes in physical condition due to illness or other causes.

Image-based video analyses have long been used in rehabilitation and other medical and healthcare fields, such as the joint research field, but it is very difficult and expensive to manage. Even if the equipment is useful, the number of people who can use it is limited [9][10]. If video analyses can be performed at a low cost, many people will be able to use it. Therefore, we examined the possibility of gait analyses by video using MediaPipe. If motion analyses

 ISBN: 978-1-61208-995-9

become possible with free software, it may become a tipping point for the rapid spread of video analyses in the medical and healthcare fields.

All research members participated in the experiment and examined the analytical data. This research was approved by the Ethics Committee of Teikyo University of Science.

II. EXPERIMENTS

The subjects were two men in their 60s and 70s, respectively. The two gait events differed in terms of ankle restrictions. The supporter restricted ankle joint motion. In the case of the elderly patient experience set, the subject wore nothing but glasses, which did not restrict ankle joint motion.

The corresponding locations of the 33 landmark data locations on the body output by MediaPipe are shown in Table I.

TABLE I. POSE LANDMARK of MediaPipe.

Pose Landmark	
0. nose	
1. left_eye_inner	4. right_eye_inner
2. left_eye	5. right_eye
3. left_eye_outer	6. right_eye_outer
7. left_ear	8. right_ear
9. mouth_left	10. mouth_right
11. left_shoulder	12. right_shoulder
13. left_elbow	14. right_elbow
15. left_rwrist	16. right_wrist
17. left_pinky	18. right_pinky
19. left_index	20. right_index
21. left_hip	22. right_hip
23. left_hip	24._right_hip
25. left_kenn	26. right_kenn
27. left_ankele	28. right_ankele
29. left_heel	30. right_heel
31. left_foot_index	32. right_foot_index

For the evaluation of Comma-Separated-Values (CSV) data from MediaPipe, the same type of pressure sensors has already been used and reported, which changes the resistance depending on the pressure, ranging from 100 to 1MΩ [7]. A 1kΩ resistor was connected in series with this sensor, and the voltage change of the resistor was used as the input signal. Each sensor measures the voltage at 1kHz. Eight sensors were arranged parallel to the direction of travel. The pressure-sensor data were connected to an Arduino Mega 2560 R3 connected to a Personal Computer (PC). The connection between the sensors and the Arduino is shown in Figure 1.

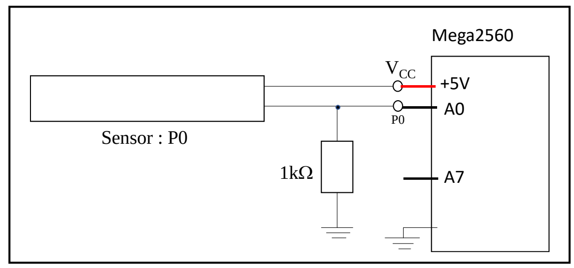

Figure 1. Connection of sensors and Arduino.

The output signals of sensor numbers A0-A7 and the distance between each sensor were used to calculate the walking speed.

A. Analysis of data obtained from MediaPipe

1) Accuracy check of CSV data outputed by MediaPipe

We investigated the possibility of using the CSV data output by MediaPipe to perform gait analysis using the elderly patient experience set. The measurement indicates how accurately the ankle position can be quantified. Because the analysis was performed during gait, we used images from the timed up-and-go measurement, which is used as a basis for the evaluation of falls in the elderly, for the analysis in MediaPipe.

Figure 2 shows the trajectory of the timed up-and-go measurement. The trajectory was similar to that of the left ankle. A detailed ankle trajectory is obtained. The video analysis of the timed up-and-go test confirmed that the maintenance of the integrity of the specifications [11]-[13]. Figure 2 shows the trajectory of the body relative to the gait site with a high degree of accuracy.

 ISBN: 978-1-61208-995-9

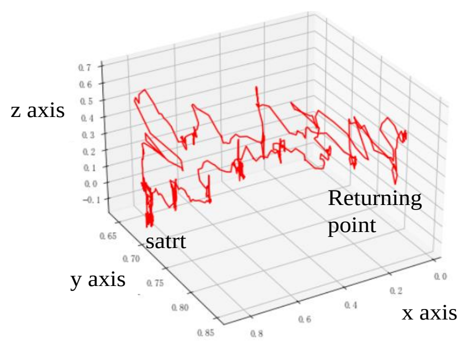

Figure 2. The trajectory of the time up and go analyzed by MediaPipe.

2) Results from the front angle

Gait videos taken from the front under two different conditions, one without motion restriction and the other with motion restriction by a knee supporter, were analyzed using MediaPipe. The left side of Figure 3 shows the image without motion restriction, and the right side shows the picture with motion restriction.

The values of z, which represent the height of the left and right ankle joints, were plotted against the presence or absence of motor restriction, respectively. The upper and lower figures show unrestricted and restricted motions, respectively.

Figure 3. The skeleton analysis of without/with restrictions using video from front.

The upper and lower figures show unrestricted and restricted motions, respectively.

The values of z in Figure 4, which represent the height of each the left and right ankle joints, were plotted against the presence or absence of motion restriction, respectively.

It can be determined that the time that the heel is on the floor is short because the average of the integrated values of the z values of the foot that is applies the restriction is large.

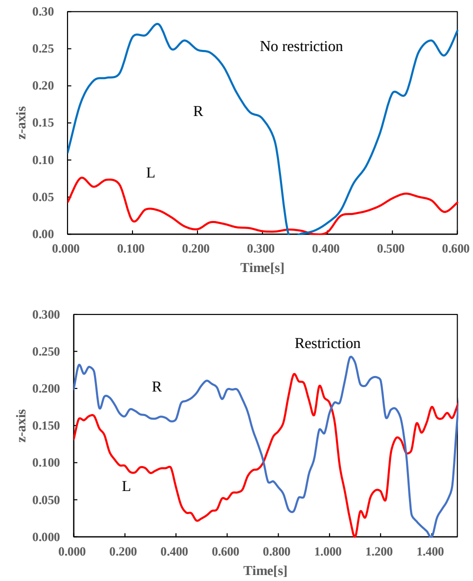

Figure 4. Values of z which represent height of ankle.

3) Results from an oblique upword angle

In this analysis, the image was taken obliquely upward, so it was enhanced by the effect of the z-axis length ratio. However, peaks corresponding to the left and right toes were also observed. Differences due to the angle of filming were analyzed from images obtained from the front and from diagonally above.

The left side of Figure 5 shows the image without motion restriction, and the right side shows the image with motion restriction. The sheet on the floor is the pressure sensors described in Figure 1 at the experiment.

Figure 5. The skeleton analysis of without/with restrictions using video from oblique upward angle.

 ISBN: 978-1-61208-995-9

The separately conducted results of the ankle angle measurements indicate that the subject's left and right feet have different flexibility. This may have a significant effect on the gait. Therefore, we considered the ankle and knee and the ankle and toes as vectors and obtained the angle between these two from the inner product. Images were taken in two different ways while the subjects were walking and being analyzed.

Based on these results, the ankle angles that significantly affected gait were determined. The results of the analysis are shown in Figure 6. The frontal view is used for images (a) and (b), and (c) and (d) are oblique images. Changes in the left and right ankle angle were almost identical with and without motion restriction. However, in both cases, the change in the right ankle angle was smaller. It is not clear whether this was a feature of the subject's gait or a software problem. Further studies are needed in another experiment with a different subject.

4) Gait speed

The gait speed was examined. As the coordinates are those of the projection from the camera, correction is necessary [14]-[17]. Although it is best to correct the coordinates from a 3D viewpoint, in this case, the correction was based on the walking trajectory. Therefore, we compared walking speeds based on measurements for which specific lengths were known.

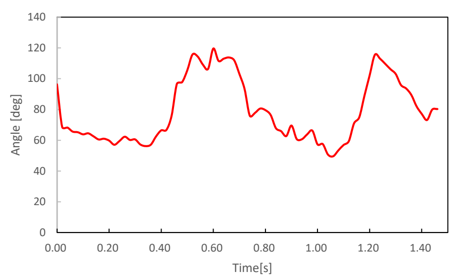

(a)

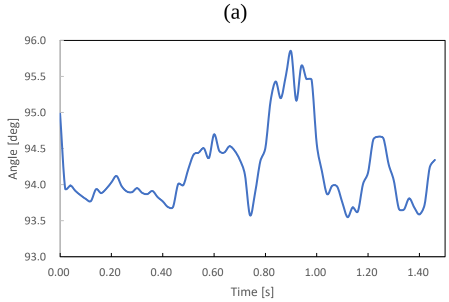

(b)

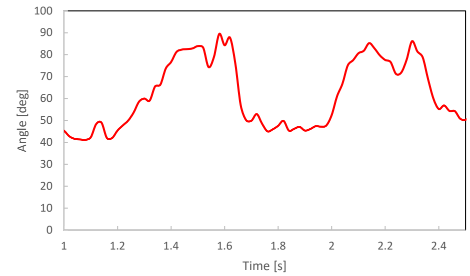

(e)

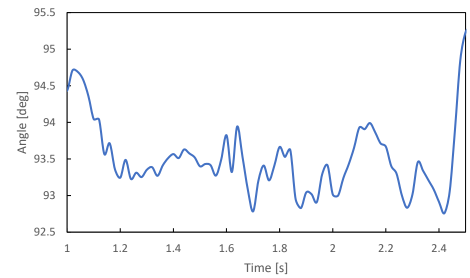

(d)

Figure 6. Results of ankle angle from the front and an oblique upward angle

As for gait speed, we also compared the data with the data from the pressure sensor and examined which points should be analyzed to obtain accurate based on the principle of the software. We determined that it would be difficult to determine the walking speed when shooting from an oblique direction because the screen is moved in an oblique direction. However, it was thought that data could be obtained for comparison if the same conditions were used. Clearly, the problem with images taken from the front was that the size of the subject varied depending on the measurement data point.

Therefore, we considered the part of the image that was considered to move as little as possible on the screen. In the present image, the shoulder area was close to the central part, therefore, we considered this point. In the walking speed obtained from walking on the mat, differences of approximately 2.1 km/h and 1.3 km/h were obtained with and without motion restriction, respectively. However, the values obtained from MediaPipe were approximately one order of a magnitude lower.

Thereafter, we plotted the data for y on the right shoulder, which had the largest slope. The right position of the shoulder as a function of time is shown in Figure 7. The obtained value was approximately 1/3 of the value. This point was examined as follows.

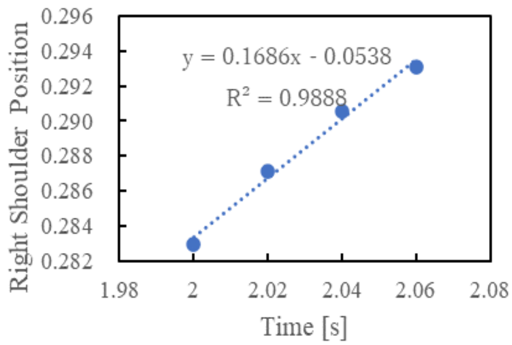

Figure 7. The right shoulder position as a function of time.

Figure 8 shows the 3D display of the trajectory of the right shoulder position. Because the slope of the change in the right shoulder position is almost 45°, it was found that using the correction value for the direction of motion on the screen, a walking speed of 0.4, which is almost the same as the 0.38 obtained from the mat, could be obtained.

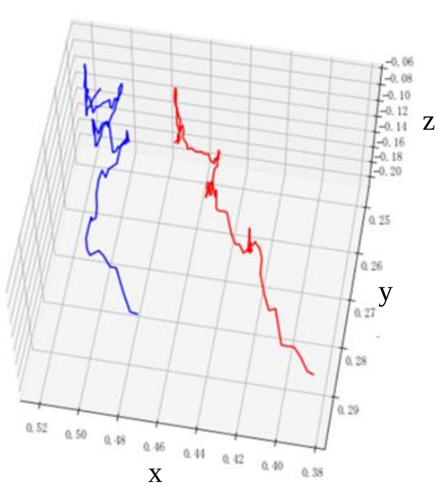

Figure 8. A 3D display of the trajectory of the right shoulder position.

The fact that walking speed can be corrected by selecting the detection point indicates that some ingenuity is needed, such as shooting parallel to the travel direction when capturing the video.

III. Discussion

The analysis using MediaPipe reproduced the left ankle trajectory in the timed up-and-go measurements as shown in Figure 2. The z-axis values corresponding to the vertical motion are small due to the screen settings; therefore, the z-axis values are emphasized. Consequently, it is necessary to make a prior reference measurement and correction for accurate evaluation. However, as shown in Figures 4 and 6, it was possible to determine the ankle angle as gait condition data, although we did not calculate this timed up-and-go measurement. Comparing the separately measured range-of-motion angle data of the ankle joint and comparative ankle joint range-of-motion angles obtained from the video, slight differences were observed due to the camera angles. The angular change in the right foot was almost the same, regardless of the camera angle. By contrast, the angular change in the left leg tended to be smaller. In the subject's gait, another measurement result showed that the joint change in the left foot was smaller than that in the right foot. It may be possible to analyze whether this is due to the subject's characteristics or the effect of the camera angle by changing the measurement conditions or by comparing the gait data on other subjects.

Because this software can be installed on tablets and smartphones, we believe we have shown that the skeleton analysis screen can be effective as a simple check at the rehabilitation site. In the case of a detailed numerical analysis, there are differences in the numerical values obtained due to differences in camera angles, necessitating the use of a camera with a sufficiently wide angle at the time of measurement or having the camera fixed to eliminate camera shake during movement. The current experiment only shows the results of the analysis of one subject with and without pseudo limitation of movement, and data from two subjects of different ages and genders measured simultaneously are currently being analyzed. Based on the above, we believe that the conditions necessary to use this software in the field can be determined by accumulating data and adapting it to subjects with gait disorders.

IV. Conclusion and Future Work

Today, with the widespread use of smartphones making it easy for many people to take videos, it is also easy to take a picture of a person's walking condition and ask a medical professional to diagnose the problem. The ability to obtain skeletal displays and numerical data, as with this software, is expected to rapidly improve the potential of video analysis in the medical insurance field.

However, the limitations of the shooting conditions when introducing this software should be considered. For example, it became clear that the shooting angle and which point the analysis should be focused on are important. We will improve the optimization of video shooting conditions and correction methods for all shooting angles. In addition, these corrections are made and adapted to the subject.

Acknowledgment

This work was supported by JAPS KAKENHI Grant Number JP20K11924.

REFERENCES

[1] L. Gonzalez-Villanueva, S. Cagnoni, and L. Ascari, “Design of a Wearable Sensing System for Human Motion Monitoring in Physical Rehabilitation,” Sensors 2013, 13, pp. 7735-7755, 2013.

[2] Y-L. Zheng, X-R Ding, C.C. Y. Poon, B. P. L. Lo, H. Zhanf, and G-Z. Yang, “Unobtrusive Sensing and Wearable Devices for Health Informatics,” IEEE Trans. Biomediacal Engineering,vol 61, pp. 1538-1554, 2014.

[3] M. M. Alam and E. B. Hamida, “Surveying Wearable Human Assitive Technology for the Life and Safty Critical Applocations: Standards, Challenges and Opportunities,” Sensors 2014, pp. 9153-9209, 2014.

[4] M. J. Deen, “Information and communications technologies for elderly ubiquitous healthcare in a smart home,” Pres Ubiquit Comput, pp. 573-599, 2015.

[5] S. Hong and K. S. Park, “ Unobtrusive Photoplethymographic Monitoring Under the Foot Sole while in a Standing Posture,” Sensors 2018, 3239, 2018.

[6] V. Bucinskas et al., “Wearable Feet Pressure Sensor for Human Gait and Falling Diagnosis,” Sensors 2021, 5240, 2021.

[7] Y. Uchida et al., “Feature Value Extraction for Body Condition Change Measurement System Using Pressure Sensor Array”Human Interface Society in Japanese, vol.24, no.1, pp. 79-82, 2022, ISSN 2188-6652.

[8] V. Bazarevsky et al., “ BlazePose: On-device Real-time body Pose tracking,” arViv:2006.10204v1 [cs.CV] 2020.

[9] P. Plantard, E. Auvinet, A. S. Le Pierres, and F. Multon,”Pose Estimation with a Kinect for Ergonomic Stuidies: Evaluation of the Accuracy Using a Virtual Mannequin,” Sensors 2015, pp. 1785-1803, 2015.

[10] J. Beyea, C. A. McGibon, A. Sexton, J. Noble, and C. O’Connell, “ Covergent Validity of a Wearable Sensors Sytem for Measuring Sub-Task Performance during the Timed Up-and-Go test,” Sensors 2017, 934, 2017.

[11] F. Buisseret et. al., “Time Up and Go and Six-Minute Walking Test with Wearable Inertial Sensor: One Step Futher for Prediction of the Risk of Fall in Elderly Nursing Home People,” Sensors 2020, 3207 2020.

[12] J. Choi, S. M. Parker, y. Gwon, and J.Youn, “ Wearable Sensor-Based Prediction Model of Time up and Go Test in Older Adults,” Sensors 2021 6831, 2021.

[13] J. P. Monteiro, A. T. Magalhaes, and H. P. Oliveira, “Human Pose Estimation, Anthropomorphism and Gamification in Promotion of Physical Activity Among Breast Cancer Surviviors,” Int’l J. on Advances in life Sciences, vol. 11, pp. 118-127, 2019.

[14] Y. Ono, O. D. A. Prima and K. Hosogoe, “Evaluation and Application of Partial Body Joint Model in 3D Human Pose Estimation from Signal Image,” Int’l J. on Advances in life Sciences, vol. 13, pp. 114-123, 2021.

[15] I. Crombrugg et al., “Accuracy Assessment of Joint Angles Estimated from 2D and 3D Camera Measurements,”, Seonsors 2022, 1729, 2022.

[16] X. Yu, J. Baar, and S. Chen, “Joint 3D Human Shape Recovery and Pose Estimation from a Signal Image with Bilayer Graph,” arXiv:2110.8472v2 [cs.CV], 2021.

[17] Z. Li, R. Zhang, C. H. Lee, and Y. Lee, ”An Evaluation of Posture Recognition Based on Intelligenct Rapid Entire Body Assessment System for Determing Musculoskeletal Disorders,” Sonsors 2020, 4414, 2020.

 ISBN: 978-1-61208-995-9

Assessment of Walking Condition Using Pressure Sensors in the Floor Mat

Tomoko Funayama
Dept. of Occupational therapy
Teikyo University of Science
Yamanashi, Japan
e-mail: funayama@ntu.ac.jp

Yasutaka Uchida
Dept. of Life Science
Teikyo University of Science
Tokyo, Japan
e-mail: uchida@ntu.ac.jp

Yoshiaki Kogure
Professor Emeritus
Teikyo University of Science
Tokyo, Japan
e-mail: kogure@ntu.ac.jp

***Abstract*— Monitoring equipment and systems for older people and those with health problems are usually based on measuring vital signs and monitoring behavior and have the problems of invasion of privacy and difficulty with operation. We have developed a floor mat-type walking measurement device with a pressure sensor to determine natural walking conditions in daily life. The equipment consisted of a grid of eight pressure sensors, each perpendicular and parallel to the direction of walking. Although walking speed was calculated using the least-Squares Method, we did not show its relevance to walking assessments. In this study, to confirm the usefulness of walking assessments with this equipment, we simulated visual and motion limitations due to weight loading on the trunk and upper and lower limbs and compared the results with the Timed Up and Go test used in rehabilitation assessments. In addition to the conventional least-Squares analysis using programming, we directly calculated walking speed by manually judging footprints and suggested key points in the calculation of walking speed. We analyzed data from the Timed Up and Go test, various movement restrictions using a floor mat-type sensor device, and normal walking with no movement restrictions. Four requirements were found to determine the calculation of walking speed, suggesting the usefulness of this device.**

Keywords-Walking Assessment; Floor mats; Pressure Sensors; Activities of Daily Living; Timed Up and Go test.

I. INTRODUCTION

The world is currently aging, with Japan having the highest rate of aging among countries. Early assessment of poor health conditions of people with health issues, including older people and people with disabilities, is useful to provide health care support. Equipment use has become an important part of providing support. Many monitoring support equipment and systems for older people and others with health problems have been developed and marketed in recent years [1]-[5]. These systems use not only video but also sensors, such as sheets, magnets, tags, ultrasound, infrared, etc., to judge problems from vital sign measurements to actions. Judgments are often based on vital sign measurements to assess health conditions and motion monitoring using video and infrared equipment. However, these have issues such as invasion of privacy and difficulty in using the device.

We have been studying monitoring systems for those with health issues and have developed monitoring equipment using a floor mat with pressure sensors [6] [7]. We then used the data from the sensors perpendicular to walking to calculate the velocity using the Least-Squares Method (LSM) and on the left and right data from the parallel sensors to perform machine learning. The key points of this equipment are twofold: privacy is ensured owing to the use of a floor mat, and health conditions are assessed without the use of vital sign measurements. In the future, it will be possible to measure the motion speed unconsciously in daily life without having to switch the equipment on and off. We have previously studied patients on dialysis using this equipment [8].

This report presents a study on the availability of the developed floor mat sensor in the rehabilitation field. We compared the results of the Timed Up and Go test (TUG), which is often used as a gait ability assessment, with those of our floor mat sensor. TUG and floor mat walking speeds were measured with the participant wearing an older person experience set to simulate motor dysfunction. In addition, an occupational therapist evaluated the video recordings and developed a new speed -calculation method. This study was approved by the Ethics Committee on Research with Humans as Subjects of the Teikyo University of Science. Section II describes the experimental methods for measurement and analysis, Section III describes the results, Section IV presents the discussion, and Section V presents the conclusion.

 ISBN: 978-1-61208-995-9

II. Experimental Method

Three subjects wore the older person experience set to measure the walking speeds in TUG and on a floor mat with grid array sensors. Walking speed was analyzed using the existing programming LSM and new methods, along with the assessment of walking by an occupational therapist. The experimental procedure is as follows:

A. Measurement

- Equipment

  The study used a floor mat with a grid array of eight pressure sensors, each perpendicular and parallel to the direction of walking. Eight sensors (P0–P7) are perpendicular to the walking direction, and eight sensors (Q0–Q7) are parallel to the walking direction (see Figure 1). Parallel sensors Q are 1.5 cm apart and are a set of two. They are arranged with four in the front and four in the back. Perpendicular sensors are 10 cm apart only at the initial P0–P1 sensor interval and 15 cm apart at the other sensor intervals. The length of the sensor was 62 cm, and it measures approximately 120 cm in the direction of walking. The equipment size allows its use and placement at home. The surface is protected by a clear plastic sheet so that the position of the sensor position can be checked. The sampling frequency of the equipment is 100 Hz.

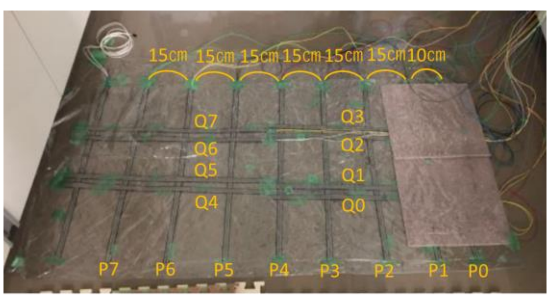

Figure 1. Floor mat-type equipment with pressure sensor array.

- Walking measurements

  Three subjects in their 50s to 70s (Cases A, B, and C) performed TUG and walked on the sensor array floor mat under simulated restricted motion while wearing the older person experience set (see Figure 2). The TUG measures the time it takes to get up from a chair, go around a cone 3 meters away, walk back to the chair, and sit down. We measured the time taken. TUG is often used in walking assessment during rehabilitation. We performed the test not only with comfortable walking, which is standard practice, but also with fast walking.

  The motion restrictions varied by subject. Subject A wore tinted eye glasses in addition to (1) trunk weighted, and left upper and lower limb restrictions, followed by (2) trunk weighted and right upper and lower limb restrictions. Subject B was (3) weighted on the trunk and had both legs restricted. Subject C was (4) weighted on the trunk.

  The subjects then walked on the sensor array floor mat without motion restrictions. Comfortable and fast walking were performed. Videotaping and ankle joint Range Of Motion (ROM) measurements were also conducted by an occupational therapist. The ROM of the ankle joint is shown in Table I, with plantar flexion and dorsiflexion. R and L represent the right and the left sides.

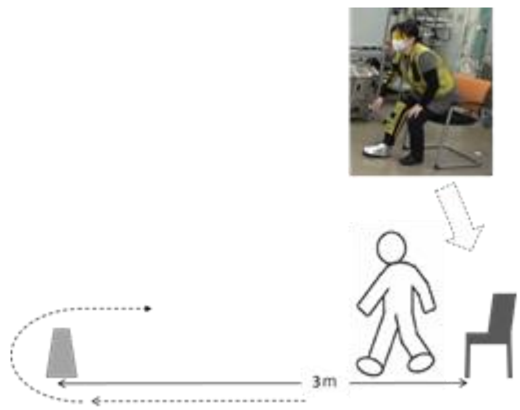

Figure 2. Timed Up and Go test.

TABLE I. Range Of Motion of cases A, B, and C

		Subjects		
Direction of motions	**R / L Side**	Case A	Case B	Case C
plantar flexion	R	50	60	45
	L	55	50	50
dorsi flexion	R	20	10	20
	L	20	5	-5

B. Analysis

- Speed calculation by the LSM

  Speed was calculated by programming using the LSM. This is the same analysis method that has already been used for patients undergoing dialysis.

$$y_i = a\, x_i + b \tag{1}$$

xi is the time when the P sensor is stepped on and yi is the distance from P0 to the stepped-on P sensor.

Figures 3 and 4 show examples of a graphical representation of the output data for P0–P7 and Q0–Q7.

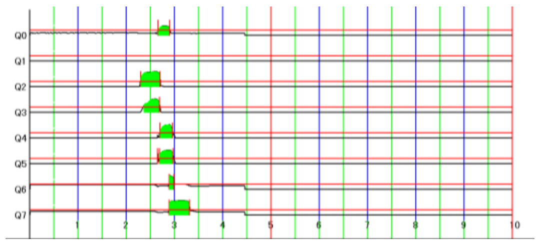

Figure 3. Q sensor output data.

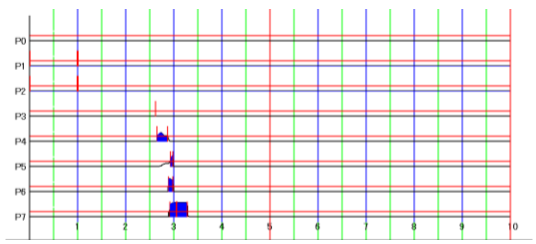

Figure 4. P sensor output data.

For the LSM calculation, data over half the height of the highest signal were used. In addition, data with very few continuous signals were judged to be noise and were not used. Figure 5 shows the time (s) and distance (sensor position), where the inclination of the red line is the speed.

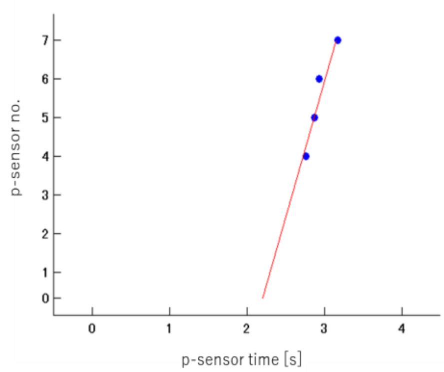

Figure 5. Speed by the least-Squares Method.

- Speed by direct calculation

A footprint diagram was drawn by looking at the raw data from the P and Q sensors, plantar ground contact was determined, and the speed was calculated (see Figure 6). When two sensors were stepped on simultaneously at the same time by a single sole, it was assumed to be a single ground contact, and the position and time that was the middle of the two sensors were used to determine the speed. It was calculated directly by manual process (Direct Calculation: DC).

The terms of judgment were as follows: (1) If there was an output that appeared to be noise that was not understood for a short time, the plantar ground contacts were judged to be grounded when 10 consecutive pieces of data were obtained. (2) Data with <2.0% of the maximum value 10 times in a row were excluded from sole grounding. (3) When two front and rear sensor data responded simultaneously, the same plantar contact was assumed when >70% of the front sensor data overlapped with the rear data. (4) When adjacent P-sensors did not respond consecutively, that is, there was one or more unresponsive P sensors in between, we assumed a different plantar ground contact.

Two major differences were noted between the LSM and DC of speed using footprint diagrams. First, the LSM calculates the speed based on the position and time of each sensor, regardless of whether the two sensors are stepped on simultaneously. The speed by the DC is calculated by judging when two sensors are outputting simultaneously, whether they are one footprint or two footprints, that is, the same grounding. Second, this is whether to use data with small values or responses in the calculation or to exclude them and treat them as noise.

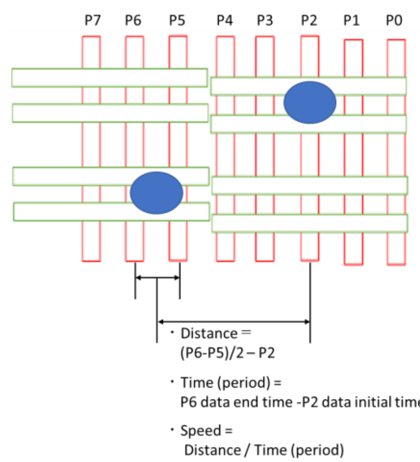

Figure 6. Footprints and direct calculation.

- Comparison with rehabilitation assessment

(1) We compared the TUG results to the sensor array data. (2) Occupational therapists assessed and validated the results by watching the video (see Figure 7).

Figure 7. Assessed video screen.

On the sensor array, subjects walked straight ahead, whereas on TUG, subjects walk straight ahead and then U-turn. The speeds on the TUG were converted and compared with the LSM and DC results on the sensor array data.

III. RESULTS

A. Speed by Calculation Method

The speed results were compared to determine the difference in the calculation method between the programming LSM and DC with footprint diagrams. Figures 8–10 represent the speed in meters per second. Data blanks in the LSM were those that could not be calculated because the number of data points was less than 2. In the graph, subjects A, B, and C correspond to 1, 2, and 3, respectively. The letters following the numbers are "Rr for right upper and lower limb restriction, "Lr" for left upper and lower limb restriction, "W" for weight loading, "E" for wearing tinted eye glasses, "c" for comfortable walking, and "f" for fast walking.

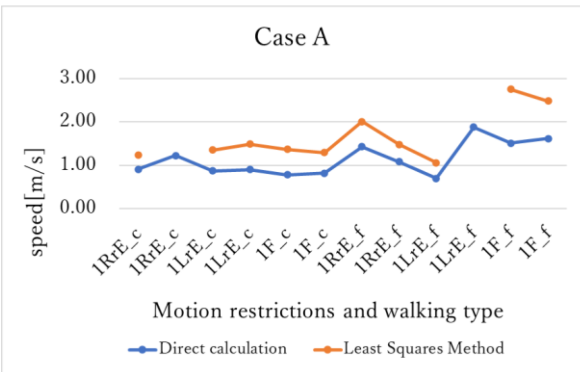

Figure 8. Walking speed by motion restrictions of subject A.

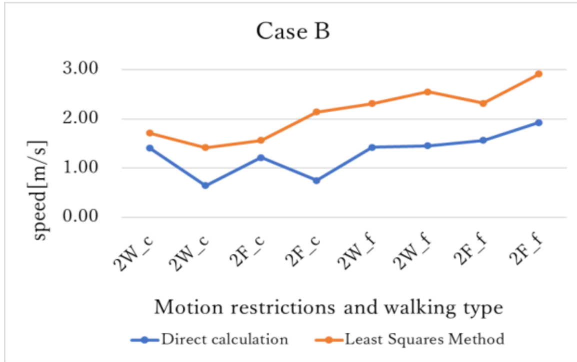

Figure 9. Walking speed by motion restrictions of subject B.

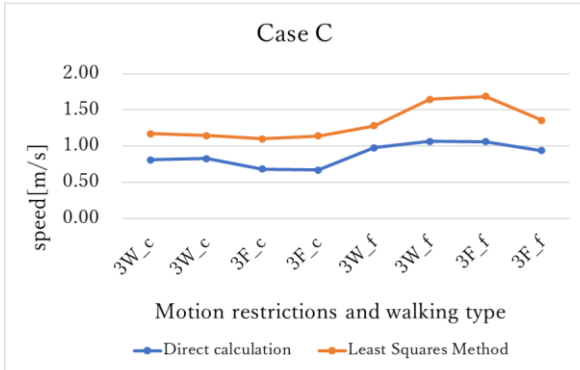

Figure 10. Walking speed by motion restrictions of subject C.

The results show that LSM tends to be judged as walking faster than DC.

B. TUG and Walking on Sensor Array Floor Mat

The speed of the TUG was compared with that of walking on a sensor array floor mat. The walking speed on the sensor-placed floor mat was calculated using two methods: LSM and DC. The mean speeds of subjects A, B, and C were calculated when they walked comfortably and fast with restricted motion. Figure11 shows the results for the TUG, LMS, and DC. The figure is graphed in ascending order of the TUG speed.

The calculation results from the pressure sensor array differed according to two calculation methods: LSM by programming and DC by manual calculation using a footprint diagram. In the LSM, the calculation result showed that the speed was slower by 3 of 7 times than the slowest speed in the "left upper and lower limbs and eye limits (1LrE_c)" TUG in Case A. In DC, the calculation result shows that only 1 of 7 times the speed was slower than the slowest speed in the "1LrE_c" TUG in Case A. The relationship between TUG and DC is higher, which is a manual calculation using footprint diagrams, than between TUG and LSM using programming. In the sensor array, walking is measured only straight ahead, whereas in TUG, walking is measured both straight ahead and U-turns. Therefore, the speed of TUG walking would be slower than that of the sensor array walking.

 ISBN: 978-1-61208-995-9

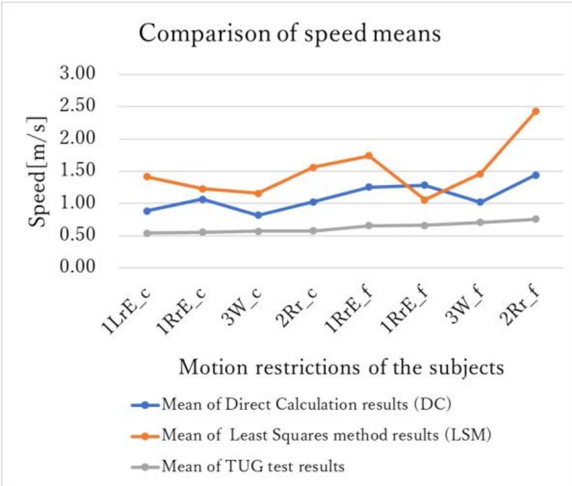

Figure 11. Speed comparison between TUG and sensor array walking.

The two discrepancies between TUG and DC were 3 W_c and 3 W_f for subject C. Subject C's walking was assessed on video by an occupational therapist, and a left-right difference was judged. Both 3 W_c and 3 W_f was observed during plantar grounding of the left foot. The ankle joint ROM in case C was R20/45 and L-5/50, with a left–right difference.

C. Judgment of Left and Right Foot Speed

The results of the speeds calculated by the DC for the simulated left and right upper and lower limb movements when restricted are shown in Figures 12 and 13, respectively; Figure 12 shows the right motion restrictions, and Figure 13 shows the left motion restrictions, x-axis is the plantar-grounded side of the foot, and y-axis is the speed. Only in case A the right and left upper and lower limbs were restricted.

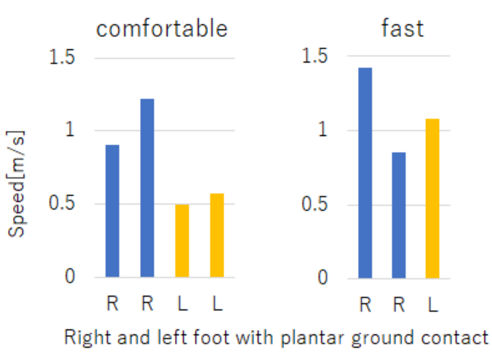

Figure 12. Right upper and lower limb restrictions.

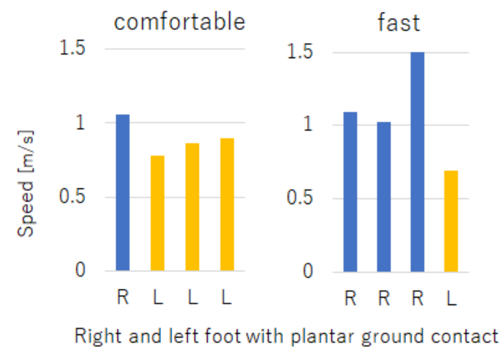

Figure 13. Left upper and lower limb restrictions.

The right-side walking tended to be faster than that of the left side regardless of whether the motions were restricted to the left or right side.

IV. Discussion

The equipment for monitoring health conditions up to now usually measures vital signs, and the monitoring care system captures movements. In this study, we used a floor mat that provides privacy while monitoring movements and enables assessment of health status based on walking patterns. However, the reliability of walking assessment using this device has not been compared with that of conventional assessments. In this study, we compared this device with TUG, which is commonly used for walking assessment. Owing to simulated motor limitations with only three subjects, it is not yet possible to generalize the results to people with disabilities. However, there was a tendency toward a relationship with conventional TUG.

In addition to the LSM of calculating walking speed that we have been using, we performed manual calculation using footprints, which showed a higher relationship with TUG. Data with low relationships were considered possibly influenced by left－right differences in the ankle joints. Footprints were created and calculated directly and manually according to the four requirements. The calculation requirements are related to whether it is a one- or two-footprint diagram, that is, the same plantar ground contact, and to determine whether data with small values or responses should be used in the calculation or excluded and treated as noise. In this study, 10 consecutive datasets were used: in the case of simultaneous response by two sensors (front and rear), the same plantar contact was considered when at least 70% of the front sensor data overlapped with the rear sensor data, but this number may vary depending on the distance between sensors and walking speed. Although the measurements were obtained with simulated motor impairment, some older people and those with disabilities were slower than others. If there is no output from the P sensor, data from the front and rear P sensors can be judged as different plantar ground contacts; therefore, it is effective to narrow the sensor interval. The LSM programming analysis was probably faster speed because two sensor data from the same plantar, that is, one footprint, were treated the

 ISBN: 978-1-61208-995-9

same way as two data from different plantar contacts, that is, two footprints. Although the speed calculated by LSM had a low correlation with TUG, it was similar to the speed calculated by manual DC. Because this study was based on a small amount of data, the correlation may be higher in the future when huge data are used for analysis in daily life measurements.

The length of the equipment was set at approximately 120 cm, which is too small for determining the walking speed. However, as the equipment can be placed at home at all times considering its size, anything larger than this is not considered practical. Even with the 120-cm equipment, differences between the left and right feet could be detected. Suppose the width of Q is narrowed so that it can automatically determine whether the left or right sole is grounded. The speed at which the left and right soles are grounded can be calculated, and changes in walking ability by left and right can be detected.

V. CONCLUSION

In this study, we investigated three subjects using a small amount of data. Therefore, the results of this study cannot be generalized. However, a relationship was suggested between TUG and array sensors, that is, the floor mat-type array sensors could be used for walking condition assessments. Occupational and physical therapists routinely assess walking conditions, but do not always use measuring devices or quantify them. They observed and assessed their interactions with the patients. Health conditions were expressed as a state of walking. If walking conditions can be measured naturally in daily life, it will be possible to assess walking ability without a therapist. This also leads to objective data showing the therapist’s tacit knowledge of experience. Motion speed measurement with pressure sensors has already been studied, as well as getting up out of the bed. The use of machine learning has also begun. We plan to study both walking and getting up from bed in the future.

ACKNOWLEDGMENT

This work was supported by JAPS KANENHI Grant Number JP20K11924.

REFERENCES

[1] M. M. Alam and E. B. Haidar, “Surveying Wearable Human Assistive Technology for Life and Safety Critical Applications: Standards, Challenges and Opportunities,” Sensors 2014, 14, pp.9153-9209, 2014.

[2] V. Bucinskas et al., “Wearable Feet Pressure Senosr for Human gait and Falling Diagnosis, Sensors 2021, 5240, 2021.

[3] J. Beyea, C. A. McGibbon, A. Sexton, J. Noble, and C. O’Connell, “Convergent Validity of a Wearable Sensor System for Measuring Sub-Task Performance during the Timed Up-and-Go Test ”, Sensors, 17, 934, 2017, doi: 10.3390/s17040934.

[4] S. Subramaniam, S. Majumder, A. I. Faisal, and M. J. Deen, “Insole-Based Systems for Health Monitoring: Current Solutions and Research Challenges”, Sensors 2022, 22, 438, 2022. doi: 10.3390/s22020438.

[5] A. Steinhage and C. Lauterbach, “Monitoring Movement Behavior by means of a Large Area Proximity Sensor Array in the Floor”, Proceedings of the 2nd Workshop on Behavior Monitoring and Interpretation, BMI'08, Conference, Kaiserslautern, Germany, September, 2008.

[6] Y. Uchida, T. Funayama, and Y. Kogure, “Suport Vector Machine Analysis to Detect Deviation in a Health Condition Monitoring System”, Sensors & Transducers, vol. 237, pp. 1-3-108, 2019.

[7] Y. Uchida, T. Funayama, and Y. Kogure, “Classification Accuracy of Suport Vector Machine, Decision Tree and Random Forest modules when Applied to a Health Monitoring with Flexible Sensors”, Sensors & Transducers, vol. 245, pp.83-89, 2020.

[8] Y. Uchida et al., “Feature Value Extraction for Body Condition Change Measurement System Using Pressure Sensor Array” Human Interface Society in Japanese, vol. 24 no.1, pp. 79-82, 2022, ISSN 2188-6652.

Estimation of Lumbar Load from Webcam Images Using Convolutional Neural Network for Standing Forward Bending Stationary Posture

Riku Nishimoto
Kochi University of Technology
Miyanokuchi 185, Tosayamada, Kami, Kochi, Japan
Kochi, Japan
email: nishimoto.riku19990917@gmail.com

Kyoko Shibata
Kochi University of Technology
Miyanokuchi 185, Tosayamada, Kami, Kochi, Japan
Kochi, Japan
email: shibata.kyoko@kochi-tech.ac.jp

***Abstract*—To prevent lumbago, it is effective to understand one's current posture situation and how to improve one's posture. Therefore, this study proposes a method to constantly observe posture and evaluate the load on the body. The realization of this method visualizes the body loads in daily life and can be used as one of the means to maintain health. Hence, this study proposes to use a web camera for sensing and deep learning as a tool for estimating body load from web image. The body load is derived using a musculoskeletal model simulation based on the skeletal information extracted from the images, and a deep learning model is prepared in advance using this as the true value. In this paper, the first subject is a stationary standing forward bending posture. The accuracy of the created deep learning model is evaluated and the results indicate that the proposed estimation method can be useful in the case of a standing forward bending posture.**

Keywords-Deep learning; Lumbar load; Musculoskeletal model simulation.

I. INTRODUCTION

Many people of all ages and genders experience lumbago, and lumbago has become a social problem because of its potential impact on daily life. Lumbago is occurred by the load associated with postural distortions. To prevent lumbago, it is useful to have a system that can improve his/her own posture. Therefore, first, this study proposes a method to constantly observe posture and evaluate the load on the body. Based on these methods, we will be developed into a posture improvement system in the future.

In our previous reports [1] [2], postures were observed using inertial sensors or optical motion capture, and noninvasive lumbar load estimation was performed using biomechanics and statistics, these estimation results confirmed a similar trend to the measured lumbar load ratio in the static posture of Nachemson et al. [3]. However, because specialized equipment and analysis are required, they are not suitable for routine observation and estimation. Hence, in this study, body load is estimated using based on data obtained from non-contact sensing method. Until now, previous researches have used skeletal detection software and deep learning from videos and images to detect the posture and motor status of children [4] [5] and falls of the elderly [6] as a method for observing daily life. In addition, several systems that use AI to evaluate posture based on skeletal position has been commercialized (Posen: Posen Co., Ltd, Sportip: Sportip, Inc.). Therefore, in this study, a web camera is used for sensing, as everyone has one and images can be gotten on a daily basis without any burden. Also, this study proposes to use deep learning as a means of estimating body load from images taking web camera. The purpose of this study is to use this estimation method to obtain body loads that can be used as a new indicator for systems that encourage voluntary postural improvement.

Figure 1 shows an overview of the proposed body load estimation system in this study. During system operation, user inputs an image of his/her posture, along with his/her height and weight, into the system, which outputs the estimated/evaluated results of the body load. To achieve this, a deep learning model is created in advance during development. In this study, the skeletal position coordinates are detected from images using AI skeletal detection software (VisionPose: NEXT-SYSTEM Co., Ltd.). After that, body load is derived using a musculoskeletal model simulation (AnyBody: AnyBody Technology) based on the skeletal position coordinates. This is used as the true value to create a deep learning model. The advantage of using AnyBody is that the various loads on the body can be obtained from a single image data set. Therefore, if dealing with a variety of body loads, create a deep learning model for each load.

The body load used in this paper is described. Previous research [7] has shown that the intervertebral disc compression force between the 4th and 5th lumbar vertebrae

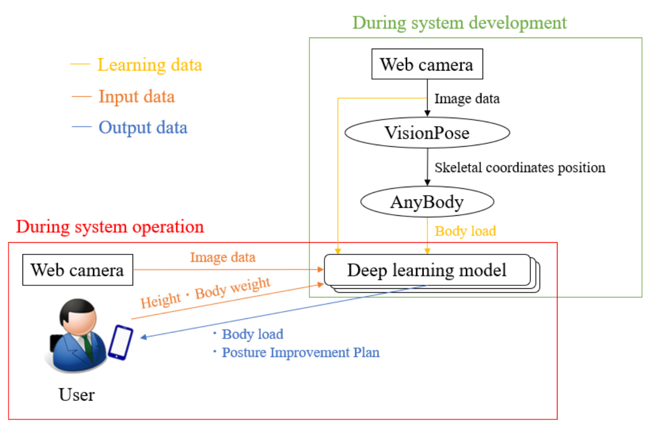

Figure 1. Overview of the proposed body load estimation system.

derived by AnyBody is useful. In response to this result, in this report, the intervertebral disc compression force between L4L5 derived by AnyBody is used as the lumbar load, which is one of the body loads. However, the input data for AnyBody is the skeletal coordinate positions of the human body. Therefore, VisionPose is used to detect skeletal position coordinates from web images. A total of 30 skeletal positions are detected by VisionPose, including hip and shoulder joints. In our previous report [8], as a preliminary step in creating a deep learning model, we confirmed whether the intervertebral disc compression force between L4L5 derived by AnyBody using the skeletal position coordinates detected by VisionPose from web images of standing forward bending posture could be used as training data for deep learning. The results confirmed its usefulness by showing an increasing trend in disc compression force with forward bending of the upper body. Hence, in this paper, we decided to use the intervertebral disc compression force between L4L5 derived by AnyBody along with the web images as the true value of the training data. In this paper, as the first step in creating the proposed system, a deep learning model is created for a stationary standing forward bending posture, and the accuracy of the lumbar load estimation by the deep learning model is evaluated. The rest of this paper is organized as follows. Section II describes the methods and conditions for creating the lumbar load estimation system proposed in this paper. Section III describes additional evaluation of the lumbar load estimation system created in Section II. The acknowledgement and conclusions close the article.

II. LUMBAR LOAD ESTIMATION SYSTEM

In this paper, we use Convolutional Neural Network (CNN) for deep learning to estimate lumbar load. This section describes the experimental methods used to collect training and validation data, the preprocessing applied to the measured data, and the training conditions for the CNN. Furthermore, the created deep learning model is used to estimate the lumbar load and confirm its accuracy.

A. Experiment

One webcam (StreamCam: logicool) is used to get video. Three male subjects (age 21±1, height 1.70±0.02 [m], weight 67.0±1.70[kg]) who gave their consent to the experiment after obtaining approval from the Ethics Committee of the University and after explaining the experiment to the subjects in advance is the subjects of this study. Subjects are unified as male in this paper because of skeletal structure differences based on gender. The camera is placed at a distance of 3 [m] from the subject's body center and at a height of 0.85 [m] from the floor. Movies are shot at 1080p/30fps. To obtain image data of random anteversion angles in the standing forward bending posture, subjects are asked to perform the following actions. The body gradually bends from an upright standing posture to about 30 degrees, then the body gradually raises to an upright standing posture. This is taken as one trial and 5 trials are obtained. A total of three videos are obtained for each subject and used as training data. In addition, one trial of video is obtained from one of the same subjects on a different day and used as data for verification.

TABLE I. CNN LEARNING CONDITIONS

		Set value
Batch size		32
Classes		120
Epoch		200
Dropout		0.2
Convolution layer	Filter size 1	32
	Filter size 2	64
	Stride	1
Pooling layer	size	(2, 2)
Fully connected layer		64

B. Estimation Methods

This study uses frame-by-frame images for learning and estimation, rather than processing on video with a time component, to estimate the posture load at a specific point in time. Therefore, the video obtained by the experiment for a total of 15 trials for 3 subjects is converted into images for each frame rate using the Python module OpenCV (image processing library). The training data totaled 3217 images, and the validation data for one trial subject totaled 657 images. Estimation uses CNN used for image classification. Numerical estimation is based on images, we consider that the same mechanism can be used for estimation as in the classification problem. The CNN structure in the deep learning model consists of an input layer, followed by two convolutional layers, one pooling layer, two convolutional layers with dropout to prevent overlearning, one pooling layer, smoothing to prevent dropout to prevent overlearning, and output to an output layer after passing through all coupled layers one layer. The Relu function is used as the activation function in the convolution layer and the Softmax function in the all-coupling layer. Keras Documentation [9] was used to create the above structure in Python. Keras.Callbacks.EarlyStopping is used as the termination condition, with the training error used as the monitor and auto as the mode. The values of each parameter are shown in Table I.

To accommodate the estimation of new subjects that will not be used for training in the future, a deep learning model is created by dividing the derived disc compression force by height and weight, normalizing it, and labeling it as the true value for each frame of training data. After that, using the deep learning model created, lumbar load estimation is performed on the validation data, and the normalized values are converted to disc compression force [N (Newton)] by multiplying by height and weight.

C. Estimation Results

To evaluate the accuracy of the lumbar load estimated by the deep learning model from each of the 657 images in the validation data, the lumbar load derived from the same validation data using AnyBody is compared with the estimated value as the true value. Figure 2 plots the estimated values from the deep learning model and the true values derived by AnyBody. Poisson's correlation coefficient r^2 is 0.997, showing a high correlation and accurately capturing the changes caused by the forward bending of the upper body. Also, the Mean Absolute Error (MAE) between the deep learning estimate and the true value derived by AnyBody was

14.7 [N]. This is 2.25 [%] of body weight, which means that the margin of error is small. Furthermore, in the next section, the results of this study will be re-evaluated through additional experiments.

III. EVALUATION METHODS

The anterior tilt angle calculated from the skeletal position coordinates detected by VisonPose is the calculated value, and the anterior tilt angle measured by a digital angle meter is the measured value. Evaluate the MAE of the deep learning lumbar load estimation shown in Section II using the error between the calculated and measured values as an indicator.

A. *Additional experiment*

Image acquisition experiment is performed to obtain the error in the upper body anterior tilt angle detects by VisionPose, and the change in disc compression force per unit anterior tilt angle derives by AnyBody. The experimental procedure is the same camera position and the same three subjects as in the experiment in Section II to obtain images in a static posture. Three pictures are taken at each of the following conditions: upright posture (0 degrees), 10 degrees, 20 degrees, and 30 degrees of upper body forward tilt angle. The forward bend angle is determined by pressing the board against the lower back and measuring with a digital angle meter.

Based on the obtained images, one is, the skeletal position coordinates indicating the body center shoulder and hip positions detected by VisionPose are used to calculate the anterior tilt angle using a trigonometric function. After that, the error is calculated from the results of the measured and calculated values. The other is, based on the images, the skeletal position coordinates are detected from each image using VisionPose, and the skeletal position coordinates are input to AnyBody to derive the intervertebral disc compression force between L4L5.

B. *Estimation Results*

Table II shows the error between the calculated and measured values of each upper body forward tilt angle, and the intervertebral disc compression force between L4L5 derived by AnyBody.

From the derivation results, it can be read that the L4/L5 Intervertebral disc load increases almost linearly in 10-degree increments. From the results, the average change in compressive force per unit angle was found to be 21.1 [N]. As described in Section II-C, the MAE for lumbar load estimation by deep learning was 14.7 [N]. This is converted into the amount of change in the upper body forward tilt angle by dividing by 21.1 [N], the amount of change in compression force per unit angle. As a result, the MAE of the lumbar load estimation by deep learning corresponds to the increase in lumbar load when the upper body forward tilt angle changes by 0.70 degrees. The average change in the upper body forward tilt angle of 0.70 degrees is smaller than the angular error detected by VisionPose shown in Table II, so the MAE of the waist load estimation by deep learning shown in Section II is small. For this reason, the deep learning model created in this paper for the standing forward bending posture is useful.

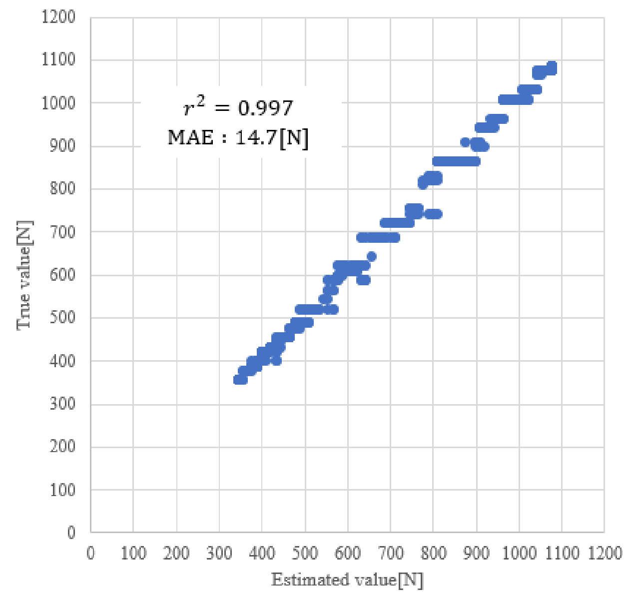

Figure 2. Comparison with disc compression force estimated by the deep learning model and the derived values by AnyBody as the true value. Presented data shows the accuracy of the deep learning model.

IV. CONCLUSIONS

The purpose of this study is to create a body load estimation system based on a deep learning model that uses web images and body load derived by AnyBody as training data. As a preliminary step, we examined the estimation of lumbar load from web images using a deep learning model that was created using the L4L5 intervertebral disc compression force derived by AnyBody as the training data for the standing forward bending posture and lumbar load, one of the body loads.

From a single image, the intervertebral disc compression forces were estimated in two different methods, one using deep learning and the other using AnyBody. In this way, the two types of forces were estimated for all validation data images, and compared with each other. The results showed high correlation and small error. Therefore, the deep learning model created in this paper for the standing forward bending posture may be useful as an estimation method for posture improvement systems.

The deep learning model developed in this paper only estimates lumbar load in the upper body forward bending posture. Therefore, the postures and their body load to be targeted by the deep learning model will be increased in the future. AnyBody can derive various body loads applied to the body from a single measured data. Hence, various body loads are obtained from a single image data, and a new deep learning model is created using this as training data. That is, it is possible to estimate selected body loads in each posture by acquiring various loads applied to each body part from images of postures that are considered to have a large load on the lumbar, such as hunching back and warped back, including the upper body forward bending posture targeted in this paper, and learning them together with the images. In addition, the

 ISBN: 978-1-61208-995-9

accuracy of the deep learning model is improved by optimizing the program through filtering and attention mechanisms. If these can be used to estimate body loads in all postures with a high accuracy, we assume that adding body loads as a new indicator to the currently commercialized posture improvement system will lead to a further increase in awareness and lead to health maintenance.

ACKNOWLEDGMENT

This work was supported by JSPS KAKENHI Grant Number JP18K11106.

REFERENCES

[1] K. Shibata, Y. Inoue, Y. Iwata, J. Katagawa, and R. Fujii, "Study on Noninvasive Estimate Method for Intervertebral Disk Load at Lumbar Vertebrae," Transactions of the JSME, vol. 78, no. 791, 2012, pp.130-141 (in Japanese).

[2] H. Himeda, K. Shibata, H. Nishida, and R. Nakata, "Study on Noninvasive Estimate Method for Intervertebral Disk Load at Lumbar Vertebrae, "The Japan Society of Mechanical Engineers Chugoku-Shikoku Branch, Student Organization, The 50th Graduation Research Presentation by Students, Lecture No. 07a2, 2020, (in Japanese).

[3] B. J. G. Andersson, R. Örtengren, A. Nachemson, and G. Elfström, "Lumbar Disc Presure and Myolectric Back Muscle Activity during Sitting," I. Studies on an Experimental Chair, Scand J Rehab Med 6, 1974, pp. 104-114.

[4] S. Suzuki, Y. Amemiya, and M. Sato, "Deep Learning Assessment of Child Gross-Motor," 13th International Conference on Human System Interaction (HSI), 2020, pp. 189-194.

[5] R. Fu, T. Wu, Z. Luo, F. Duan, X. Qiao, and P. Guo, "Learning Behavior Analysis in Classroom Based on Deep Learning," Tenth International Conference on Intelligent Control and Information Processing (ICICIP), 2019, pp. 206-212.

[6] M. D. Solbach, and J. K. Tsotsos, "Vision-Based Fallen Person Detection for the Elderly," CoRR, abs/1707.07608.

[7] T. Bassani, E. Stucoviz, Z. Qian, M. Briguglio, and F. Glbusera, "Validation of the AnyBody full body musculoskeletal model in computing lumbar spine loads at L4L5 level," Journal of Biomechanics vol. 58, 2017, pp. 89-96.

[8] R. Nishimoto and K. Shibata, "Estimation of Lumbar Load from Webcam Images Using Musculoskeletal Model Simulation," The Japan Society of Mechanical Engineers Chugoku-Shikoku Branch, Student Organization, The 50th Graduation Research Presentation by Students, Lecture No. 05b2, 2022, (in Japanese).

[9] Keras Documentation, https://keras.io/ja/, retrieved: August, 2022.

TABLE II. MEAN ABSOLUTE ERROR BETWEEN CALCULATED AND MEASURED VALUES AND INTERVERTEBRAL DISC COMPRESSION FORCE BETWEEN L4L5 AT EACH UPPER BODY FORWARD TILT ANGLE.

Upper body forward tilt angle [degrees]	0	10	20	30
MAE of angle [degrees]	2.17	2.58	4.58	3.46
L4/L5 Intervertebral disc load [N]	365	584	798	998

 ISBN: 978-1-61208-995-9

Building Mental Resilience through Online Interactive Learning for Students in Higher Education

Zi-Ying Chong[1], Ah-Choo Koo[1], Hawa Rahmat[2]
[1]Faculty of Creative Multimedia
[2]Faculty of Applied Communication
Multimedia University
Cyberjaya, Malaysia
Email: 1221400561@student.mmu.edu.my, ackoo@mmu.edu.my, hawa.rahmat@mmu.edu.my

***Abstract*—The global pandemic of COVID-19 has brought significant changes to the academic life of higher education students. Many of them face stressful and challenging situations, which calls for the need of resilience. The awareness, identification and practice of resilience traits are beneficial for students and this learning aspect is often not being taught within the university courses. The objectives of this paper are: 1) To review resilience models and identify resilient traits from the models, 2) To propose a study of online resilience building for higher education students using interactive tools and online modules. Three different models were reviewed to help building academic resilience. Some key traits of resilience are identified from the models, and to be included in the online interactive learning and modules in "Resilience Building" Knowledge Programme for higher educations.**

Keywords- Interactive learning; online module; resilience building; interactive tool.

I. INTRODUCTION

In the digital era where cybercultures took over the world, their related technologies became a part of our daily life. Devices and gadgets are becoming more and more accessible with the development of technologies. Students in higher education institutions are exposed to information overload, fake news, and infodemic perspective, which has the effect of diverting their attention away from their studies. As this happens, industries, such as medical, education, and manufacturing each have multimedia tools developed for different purposes and to meet different needs. One of them was the need to improve mental well-being or wellness of the talents in these industries.

Since the COVID-19 pandemic outbreak, countless students worldwide were led into a new mode of study. Instead of physical and face-to-face classes, hybrid and online modes of study have emerged as new mainstream modes of study. This brings the students into a distressing situation, which calls for inner mental strength to adapt to this ever-changing world, and resilience became a valuable quality for students to succeed in a challenging situation. Alongside the adaptive strategies in maintaining normal work and school life in midst of the pandemic, industries and tools that provide online learning platforms, such as Zoom and Google Workspace also flourished. This opens an opportunity for educators to convey their message and teaching resources in a more accessible way, which would benefit learners and future talents regardless of their locations. Previous Resilience Building Programme were mostly in-house and face-to-face within an institution. With online and interactive technologies as an enabler, this study explores open concepts of Resilience Building Programme for wider access to students in higher learning institutions.

Section II introduces the background of the proposed study, the challenges faced by higher education students in the post pandemic era, and the key concepts of the study are highlighted. Section III starts to address the first objective of the paper by briefly reviewed the three resilience related models, which can contribute to a robust guide of resilience modules, and finally Section IV addresses the second research objective by proposing a study on Resilience Building Programme to be recommended for higher education students. The last section concludes the paper.

II. RESEARCH BACKGROUND AND CONCEPTS

A. *Online and Interactive Learning*

Online learning is an educational concept that was brought up over two decades ago. It can be defined as an alternative way of study, mainly at the tertiary education level, and is often referred to as e-learning as well. It is also an umbrella term for learning process that took place across distance instead of in traditional classrooms [1].

Interactive learning is a type of learning that required and encouraged student participation and engagement during the teaching process. Instead of lectures, students are encouraged to explore and learn through interactive learning environment with the presence of instructors, peers and materials. It can be a problem or project-based learning and sometimes requires discussion and sharing. This type of learning method also incorporated multimedia tools such as, videos, websites, games, and applications to bring the learning process into another dimension and increase engagement. This environment is open, virtual, regardless of geographical location, and time.

During the COVID-19 outbreak, universities and schools are required to adhere to the government's constrain on order and policy. Through the phase of quarantines, both modes of learning were used more often than ever. Students were required to adapt and have classes, tests, quizzes, and submit assignments online. In a situation where social contact is discouraged, interactive learning was the main tool that students rely on for their learning and developments. The concept of a virtual classroom was widely known among students and the practice incubates tools and applications that aid such a learning mode. The changes were revolutionary as the mentioned mode of learning has been more accessible than ever. Video conferencing and interactive tools such as, Zoom, Kahoot, and Google Classroom have become a crucial part of a student's study life. Utilizing such tools also provided convenience to the process of training and learning and made the processes more convenient for some, as traveling or commuting is not required. It is also a mode of study that ease social anxiety as students felt more secure and would be more willing to share and interact with instructors [2].

B. *Students' distress and related issues*

Among the common stressors of a student are academic responsibilities or pressures, finances, anxiety, poor work/school-life balance, and family issues. On top of the already stressful tertiary education, students learning during the pandemic was also isolated and faced the fear of contracting the COVID-19 virus. The fear of going unemployed after graduation also rose as work situations also revolved in a different mode during the pandemic. The spreading of fake news is another fear that cannot be taken for granted. The Malaysian Communications and Multimedia Commission's (MCMC) findings on the propagation of fake news about coronavirus mortality is concerning in our culture [3]. This is because irresponsible people's attitudes provoke panic and concern in those who lack reputable sources of viral knowledge and are readily duped. They disseminated the fake news via various social media platforms such as, WhatsApp groups, family, community, and so on. A reasonable person should be able to verify their legitimacy by visiting more accurate websites, such as, the Ministry of Health Malaysia's website, MySejahtera or their social media channels. Amidst all the stress and fears, one might face psychological issues such as, anxiety, depression, and even develop eating disorders. This leaves a negative impact on students' academic performance and further discourages them from achieving their potential [4].

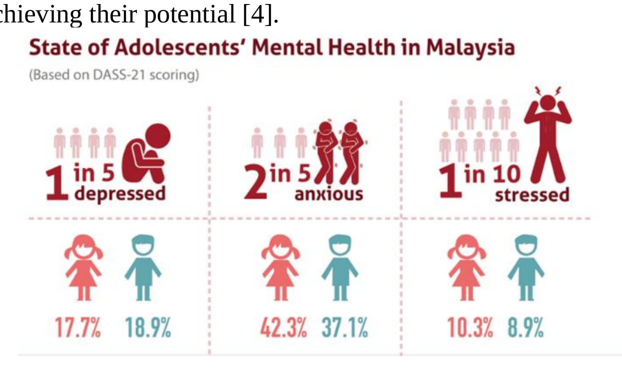

Figure 1. Statistics show the mental health conditions of adolescents in Malaysia [5].

The statistic in Figure 1 shows that Malaysian adolescents aged 13-17 experienced depression, anxiety, and stress. Among them, anxiety was the most significant issue as 2 out of 5 faced it with 42.3% of females and 37.1% of males.

C. *Mental Well-being and Resilience in Academic Settings*

Resilience can be defined as the capacity to recover or bounce back from difficulties and challenging situation. The American Psychological Association once defines resilience as "the process of adapting well in the face of adversity, trauma, tragedy, threats or even significant sources of stress." [6] In the situation of trauma and stress, such as financial problems, death of a loved one, due dates and failure, calls for this quality to strengthen one's inner strength and determine their strategy to overcome hardships. In a student's reality, resilience can differ in multiple degrees across their domains of life as they play their role as students, children, or employees. Developing resilience would help said students maintain a healthy, stable, and functional mental state after an adverse event or amidst challenges of academic life. Students could greatly benefit from having a tailored program to foster resilience or mental strength within them as an aid to support their identified challenges.

On the other hand, mental well-being is a term often associated with resilience. Being in a state of good mental well-being keeps students thriving in various areas of life, such as, interpersonal relationships, academic performance, and work. Being in a mentally well state is in fact not equivalent to the absence of mental illness or adversity but acknowledging and believing the said problems can be handled and healed. This resonates with the concept of resilience and hence resilience is one of the qualities that ones can enhance their mental well-being.

The qualities of well-being and resilience are vital for students to face their academic challenges and stress. By acquiring them, students can have the chance to display their potential in academic settings. This helps them to gain control of their life and to build soft skills, which would, in turn, help them adapt to the work environment after graduation. These qualities are believed to be a learnable skill or trait to help them flourish despite facing tumultuous situations.

D. *Interactive learning*

Interactive learning is a type of learning method that encourages learning exchange and independent study with the aid of interactive tools and means such as, the Internet, website, games, and applications. It requires hands-on activity or approaches for the students to build engagement and learn a certain topic. It can be conducted through guided activities or interactions with various tools [7].

E. *Online Modules*

The term module is often used to describe unit or lessons. It breaks down knowledge into digestible, smaller pieces with a clear progressive path to build understanding on a field or skill. Online course or modules can be defined as a web-based learning experience in which students are able to access to teaching materials via online or multimedia tools such as, audio or video [8]. Online modules are designed for students with academically sound content that is devoid of incorrect information or fake news.

 ISBN: 978-1-61208-995-9

F. *Interactive tools*

An interactive tool is a method to induce engagement within a targeted audience or user by providing them with functions within webpage, application, or other multimedia tool that users can interact at their own pace. It can also contain information, have different functionalities or assessment, and with an educational purpose. It is also widely used in fields that require huge amount of skill training and simulations [9].

III. Resilience Building Models for Students' Well-Being

A. *The Need of Building Resilience for Students*

Students faced different stressors on academic aspects, which included due dates, assignment workload, and peer pressure. To face these stressors, students can benefit themselves by building resilience. However, resilience building is not officially taught in many university course modules. To have academic resilience as a student means to face challenges with a never giving up attitude, able to bounce back from a failed attempt, and eventually drive themselves towards success. This also allows students to have capacity to perform better even in a disadvantaged background. This helps students to be a high achiever in academic background.

Resilience building is a crucial part of training for students. They should be exposed to various resilience models. Three resilience models are reviewed as follows:

B. *The 5-Part Model of Resilience*

The 5-part model of resilience would be the theoretical foundation of research and training for students (refer to Figure 2). It consists of five components that "represent the interaction of an individual's environment, thoughts, feelings, behaviors, and physical reactions" [10], which was also the pillar of building resilience.

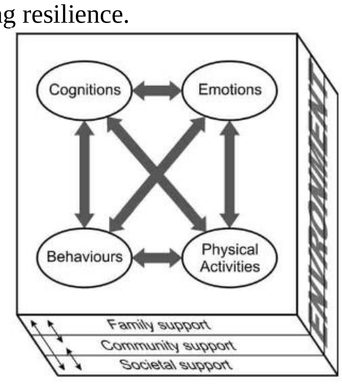

Figure 2. The extended five-part model of resilience [10]

These pillars were used to understand the past experience of individuals in cognitive behavioral therapy, especially those who suffered in distress or adverse events. Through this, resilience is investigated as a multidimensional concept that was built up from personal, social, and physical resources. The concept of this resilience model was first brought up in the 1999 by Kumpfer and included some internal and external aspects. This 5-part model was an updated one that recognized the key part in internal and external aspects while broaden the environmental factors such as, family, community and societal support on top of the five identified pillars of resilience.

This model would be a guide to students' internal aspects, which were cognitions, emotions, behaviors, and physical activities as well as their external factor, the environment. Cognitive aspect was how individuals interpret the situation they faced and their outlook on it. Emotion describes the feelings and thinking style, which have an impact on individual's mood and thoughts. Behavior describes the reaction and action individuals take and utilize in different situations. This is not to be confused with physical activities, which was the physical sensation that individuals experience. It could be non-autonomous such as, anxiety, nausea and shortness of breath though it can be controlled by consciously managing it through rest and relaxation. Through understanding these aspects and how they worked, resilience and what foster it can be understood to help those students who wish to acquire resilience as their own trait [10].

C. *The 5R model*

The 5R model is a framework proposed by Global Health Connect (GHC) [12] which is formulated based on the psychosocial foundations that can enhance well-being and productivity at workplaces. This model creates mental health awareness based on Resilience, Relationship, Roles, Respect and Resolution. It is believed that this mental health 5R model will be useful for students as well to improve their resilience, focus, relationship with others and well-being. This model is applied in the GHC's psychosocial interactive mobile application for workforces, named as Empathic.

It encompasses 5 aspects, which the first aspect is resilience, as it is critical to overcoming stressful situations in any type of work environment. The relationship is a factor that provided psychological safety and assure success and achievements. Roles can provide clarity to goals and ensure an undisrupted workflow and keeps the working process efficient. It also improves the sense of satisfaction as individuals contribute to their own roles. This model also included resolution which is a sense of purpose and meaning that drives people forward. The final aspect of this model is respect that aimed to reduce interpersonal conflicts, especially when mingling in a diverse culture [12].

Introducing students to this model would be an aid for the students to observe their current situations from different dimensions and viewpoints thus making their decision based on better judgement.

D. *The PERMA model*

This model was introduced by Martin Seligman [13] as an evidence-based approach to achieving a happy state and decreasing the likeliness of anxiety, depression, and stress. This model included many activities to systematically improve individual's positive emotions (P), engagement (E), relationships (R), meaning (M), and achievement (A), which fits in the PERMA abbreviation.

This model pursues the concept of happiness and well-being through said five aspects. It describes the significance of optimism in life, relationships, and situations. It also introduced the flow state where one is fully involved and enjoying what they do while getting rewarded with efforts made. This model also states the sense of belonging is a key to well-being and isolation and loneliness in a relationship often do harm to one's mental well-being. Living a meaningful life with a sense of accomplishment also contributes to a state of happiness as well [14].

The concept of happiness and positive psychology would bring students to the attention of the importance of consciously managing and reaching for their happiness through positive thoughts and choices.

E. Instilling Traits of Resilience for Students

To possess the traits of resilience with improved mental well-being, students should acquire a few traits of resilience based on the three reviewed models. According to the 5-part model of resilience, students should have a positive view to themselves in terms of their ability and potential. They should also have stable emotion and consciously manage their thinking and behavior in a healthy and positive way. This also resonates with the concept of PERMA, which encourages the students to find and manage happiness in what they do. These two models will help in training students to have a positive attitude when facing challenges, bounce back from failure, and build up confidence gradually. This practice encourages students to face challenges and stress with a changed attitude and hopefully found success of their own way. The 5-R model provides a dimension for students to recognize the importance of being resilient for them in academic life with continuous assignments or projects to be accomplished. Students' apprenticeship and work-life balance should consider the tenets of 5Rs, to be more comprehensive for building their resilience. Furthermore, students can also consider to get help or support from others when trauma and stressors are overwhelming. A resilient student will be able to use all the internal and external strength they have with intention to succeed in what they do. This would mean that they are determined to achieve goals even when facing setbacks and failure. This will also help them cope with negative situations and emotions. They need to manage their strong emotions and consciously stay in a healthy thinking style that encourage them to never give up.

An online course was conducted to participants consisted of university students from the UK. Each was given rating of happiness each week where, on average, happiness ratings significantly increased throughout the course [15] (refer to Figure 3). The study found that the first-year university students took the same online course during their first term experienced positive benefits to mental well-being in comparison to the control group who were the wait-list group. Hence online based training can be a promising external support for students to improve their mental well-being and resilience.

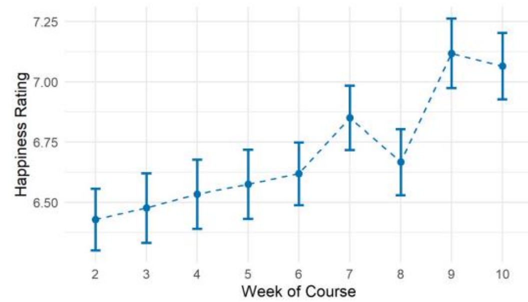

Figure 3. Statistics shows the rating of students' happiness increase over the course of 10 weeks

By using an online approach, students can feel secure by keeping their identity a secret when they share experience and receive help. The location will also not put as a constraint for students to get help.

IV. Resilience building Knowledge Programme for students in higher education: A proposed study

This section is to address the second objective of this paper. A study is proposed with the aim to examine whether an online interactive module of resilience is able to improve final year students' awareness of resilience, its traits and the coping strategies in their attempt to achieve academic performance.

For undergraduate students, their final year was the most crucial year for them to build employable skills as they will eventually graduate and join the workforce. This is also the year that students will face most of their academic challenges and would greatly benefit from Resilience Building Programme. Hence this research will also review some resilience models currently available, which would aid the students in pursuing their academic success.

This would help them to thrive in their higher education studies and achieve academic goals. With the awareness of maintaining and managing their mental well-being for a more resilient self, students can be guided to acquire the quality of resilience to navigate themselves to success. This would be done by focus group discussion with the targeted students.

The students will be requested to fill two instruments regarding their mental well-being and resilience. The instruments involved are the Kessler Psychological Distress Scale (K10) and The Utrecht Work Engagement Scale for Students (UWES–9S), which carries ten and nine items respectively to collect quantitative data for this research. K10 provided a brief screen and aided in identifying the level of distress among the selected students. This scale is highly reliable despite its simplicity [16]. The Utrecht Work Engagement Scale for Students (UWES–9S) measures the levels of energy and mental resilience in the process of working. It also investigates the sense of significance, inspiration, pride, attitude towards challenges, and concentration in work [17]. They will then be guided through an interactive module online based on the three models stated before to help build their resilience. The K10 and UWES-9S instruments will be filled before and after the module as comparison. Data collected will be computed and analyze for group comparison. Interactive tools such as Google Meet, Empathic application and website will be used in this module. The contents of the module will consist of and backed by the three models, the 5R, PERMA, and the 5-part resilience model in order for them to acquire the traits in these models. Data collected will be used to design a resilient building application aimed to build resilience among higher education students. This study will take approximately a year.

The significance of the study is that when resilient building for students can be done easily in terms of location and cost, it can be accessible for many students, and they are able to get a fair chance to be successful in academic life. Students' dropout rate and complications caused by academic stress can be reduced simultaneously.

V. Conclusions

This paper highlighted some key concepts of research to be proposed and carried out in a study. The goal of research is to improve awareness and possibly to build resilience and well-being of students in higher education. The study will utilize online learning, interactive tools, video conferencing tools and online modules for reaching to a wider group of students.

Resilience building for younger generation is urgent and important, especially those who are studying in the technical domains and vulnerable of information loading with low Internet literacy level. Soft skills on resilience awareness and learning should be widely introduced to benefit more young learners. Moreover, the skills may assist them in remaining attentive of any material loaded on the internet elsewhere. They are supposed to choose and filter the suitable information that is loaded to them.

Online learning, Resilience Building module, interactive learning and engagement should be the next agenda of higher education, so that the graduates produced are resilience in facing greater challenges in their life and works.

Acknowledgment

This research is supported by the Malaysia Ministry of Higher Education's Fundamental Research Grant Scheme (FRGS) [FRGS/1/2020/SS0/MMU/02/8].

References

[1] V. Singh and A. Thurman, "How many ways can we define online learning? A systematic literature review of definitions of online learning (1988-2018)", American Journal of Distance Education, vol. 33, no. 4, pp. 289-306, 2019. Available: 10.1080/08923647.2019.1663082. [Retrieved: September 2022].

[2] Z. Jing, S. Lu, J. Turi, and A. Warda, "Learning online sustainable education projects and students behavioral intentions during COVID-19", Tobacco Regulatory Science, vol. 7, no. 5, pp. 3543-3558, 2021. Available: 10.18001/trs.7.5.1.132. [Retrieved: September 2022].

[3] Malaysian Communications and Multimedia Commission (MCMC) Portal. Retrieved March 2020 at https://www.mcmc.gov.my/

[4] I. Rodrigues, T. Nunes, C. Cortez, and A. Lourenço, "E-learning impact on veterinary medical student's mental health during the COVID-19 pandemic", Journal of Veterinary Medical Education, p.e20210052, 2022. Available: 10.3138/jvme-2021-0052. [Retrieved: September 2022].

[5] Institute for Public Health (IPH), "Institute for Public Health (IPH)'s National Health and Morbidity Survey (NHMS)", Institute for Public Health (IPH)', Setia Alam, 2018. [Retrieved: September 2022].

[6] E. Dean, "Resilience: what it is – and what it isn't", Nursing Standard, vol. 36, no. 11, pp. 39-39, 2021. Available: 10.7748/ns.36.11.39.s20. [Retrieved: September 2022].

[7] X. Xia, "Sparse learning strategy and key feature selection in interactive learning environment", Interactive Learning Environments, pp. 1-18, 2021. Available: 10.1080/10494820.2021.1998913. [Retrieved: September 2022].

[8] A. Brel, A. Artyukhina, N. Tankabekyan, N. Skladanovskaya, and E. Zhoglo, "Bite-size learning as a strategic format of modular online learning", Современные проблемы науки и образования (Modern Problems of Science and Education), no. 52021, pp. 49-49, 2021. Available: 10.17513/spno.31167. [Retrieved: September 2022].

[9] F. Elkhamisy and A. Sharif, "Medical students perceptions of virtual learning stations as an innovative teaching tool: a qualitative study", Interactive Learning Environments, pp. 1-17, 2021. Available: 10.1080/10494820.2021.2002366. [Retrieved: September 2022].

[10] I. de Terte, J. Becker, and C. Stephens, "An Integrated Model for Understanding and Developing Resilience in the Face of Adverse Events", Journal of Pacific Rim Psychology, vol. 3, no. 1, pp. 20-26, 2009. Available: 10.1375/prp.3.1.20. [Retrieved: September 2022].

[11] B. Stoliker, A. Vaughan, J. Collins, M. Black, and G. Anderson, "Building personal resilience following an online resilience training program for BScN students", Western Journal of Nursing Research, vol. 44, no. 8, pp. 755-764, 2021. Available: 10.1177/01939459211017240. [Retrieved: September 2022].

[12] Globalhealthconnect.co, 2022. [Online]. Available: https://www.globalhealthconnect.co/empathic. [Accessed: 06-Sep- 2022].

[13] M. Seligman, Flourish: A Visionary New Understanding of Happiness and Well-being. Free Press, New York, 2011

[14] A. Mayo, E. Velaz, N. Nieto, and P. Sánchez, "Working happiness in the human resource of a university organization based on Seligman's PERMA Model", International Journal of Human Resource Studies, vol. 9, no. 4, p. 101, 2019. Available: 10.5296/ijhrs.v9i4.15718. [Retrieved: September 2022].

[15] C. Hobbs, S. Jelbert, L. Santos, and B. Hood, "Evaluation of a credit-bearing online administered happiness course on undergraduates' mental well-being during the COVID-19 pandemic", PLOS ONE, vol. 17, no. 2, p. e0263514, 2022. Available: https://journals.plos.org/plosone/article?id=10.1371/journal.pone.0263514. [Retrieved: September 2022].

[16] M. Smout, "The factor structure and predictive validity of the Kessler Psychological Distress Scale (K10) in children and adolescents", Australian Psychologist, vol. 54, no. 2, pp. 102-113, 2019. Available: 10.1111/ap.12376. [Retrieved: September 2022].

[17] M. Carmona-Halty, W. Schaufeli, and M. Salanova, "The Utrecht Work Engagement Scale for Students (UWES–9S): Factorial validity, reliability, and measurement invariance in a Chilean sample of undergraduate university students", Frontiers in Psychology, vol. 10, p.1017, 2019. Available: 10.3389/fpsyg.2019.01017. [Retrieved: September 2022].

3D Flickers for Visually Evoked Potentials-based Brain Computer Interface Paradigm in Virtual Reality

Thibault Porssut
Altran Lab
Capgemini Engineering
Paris, France
0000-0002-6691-1427
email: thibault.porssut@capgemini.com

Alix Gouret
Altran Lab
Capgemini Engineering
Paris, France
email: alix.gouret@capgemini.com

Solène LeBars
Altran Lab
Capgemini Engineering
Paris, France
email: solene.lebars@capgemini.com

***Abstract*—One of the most commonly used non-invasive Brain-Computer Interface (BCI) paradigms for virtual reality control relies on particular brain signals: Visually Evoked Potentials (VEP). However, the optimization of virtual 3D targets is required in order to conciliate satisfying VEP induction - leading to high classification accuracy - and visual discomfort minimization. This constitutes a real challenge that could unlock new possibilities for rehabilitation, gaming or other applications. In the current experiment, we designed 30 original 3D-stimuli by combining particular visual patterns with various 8Hz-movements. The objectives were (1) to test new associations of stimuli for better BCI-VR(Brain Computer Interface- Virtual Reality) ergonomics and (2) to test a new paradigm of VEP-based BCI that discriminates stimuli according to their visual features (e.g., motion type) without exploiting any variation in flickers' frequency (constant frequency = 8Hz). Offline classification abilities were assessed using an EEGNet deep learning model. The results suggested the possible role of the stimulation patterns on the visual fatigue induced. The EEGNet model successfully classified all the 30 stimuli with a high level of accuracy (97.58%). This development broadens VEP-BCI stimulation possibilities and could allow overcoming the problem of epileptogenic frequencies by exploiting visual properties of targets instead of frequency variations to discriminate VEP-BCI stimuli.**

***Index Terms*—VEP, SSVEP, BCI, VR, EEGNet, Deep Learning.**

I. Introduction

There is great potential in combining Virtual Reality (VR) with non-invasive Brain-Computer Interface (BCI) within gaming and clinical fields. Visual Evoked Potential based BCI (VEP-based BCI) constitutes one of the most efficient BCI paradigms for this kind of interaction. VEPs correspond to brain activations in visual areas, which are often induced by flickering stimuli / beating effect, and which can be measured via electroencephalography (EEG). In VEP-based BCIs, subjects must shift their gaze and attention to flickering stimuli. A strong correlation between the flicker frequency and the electroencephalogram pattern can then be observed [2]. Two main types of stimuli are usually used to elicit VEP: frequency modulated VEP (f-VEP) and pseudorandom code modulated VEP (c-VEP). In the f-VEP-based BCI paradigm, stimuli flash at different frequencies and elicit periodic sequences - Steady-State Visual Evoked Potential (SSVEP) - of evoked responses with the same spectral characteristics (fundamentals and harmonics) as those of the stimulus [3]. The main advantages of this method are the stable characteristics of the signal, the high information level and accuracy [2], [26], and a good user experience (control and intuitive) [19], [24].

In the c-VEP-based-BCI, a pseudorandom sequence is repeated periodically, modulating the stimulus appearance and eliciting specific patterns in the electroencephalogram. This method requires a higher information rate and enables high-speed BCI [3]. Although VEP-based BCI can be very efficient, the flickering aspect might cause visual fatigue, and the VEP features depend on stimulus characteristics, which are limited by the refreshing rate of the system [2]. Thus, stimuli choice represents a major limitation of VR-BCI. Visual fatigue here refers to the state of reduced alertness and the feeling of tiredness which both impair the willingness and ability to perform a task [4], [8], resulting from visual stimulations.

In f-VEP-based BCI, different paradigms have been proposed to minimize performance decrease due to repeated visual stimulation. Those paradigms regard both the stimulation graphics (visual aspect such as shape, color, pattern) and the periodic motion (frequency, waveform, motion evoked potentials) [6], [7], [10], [12], [23]. For example, steady-state motion VEP paradigm has been proposed as an alternative to that of SSVEP to reduce visual fatigue while ensuring a comparable level of accuracy [5], [12], [14]. However, very few studies have compared stimulation modalities and paradigms in a VR environment yet [7]. Moreover, most did not take advantage of VR characteristics by displaying 2D targets on plain walls for instance.

Given the lack of literature on the combination of VR and BCI, and especially on using 3D objects to elicit visually evoked potentials, the combinations of VEP stimulation paradigms were investigated (with both c-VEP stimuli and f-VEP ones – SSVEP and Steady-State Motion Visual Evoked Potential (SSMVEP)). These new paradigms might overcome

 ISBN: 978-1-61208-995-9

the visual fatigue induced by the beating effect of standard flickering stimuli while offering high classification performance. Thus, first, new 3D ergonomic flickers were proposed. Then, the 3D flickers were evaluated within a VR environment through ergonomics ratings and EEG signal quality. Finally, the last objective was to discriminate flickers based on their specific visual features and not their frequency, which remains constant (8Hz).

The rest of the paper is structured as follows. In Section II, we detail the experiment design and the methods. In the section III, we present our results. Finally, we conclude the work in Section IV.

II. Materials and Methods

A. Participants

Twenty-four participants consented to take part in the study. They had normal or corrected vision and were either naïve or had already experienced standard VEP stimulations (flickering objects) or VR. Data from twelve participants could not be included in the study due to technical problems or interruption of the experiment.

B. Equipment, Software and EEG Pre-processing

Participants were equipped with a Pico Neo 2 Eye, a Head-Mounted Display (HMD) with 3840x2160 pixels per eye at 75 Hz refresh rate. It has a Field of View (FOV) of 101° (diagonal) (see Figure 1). The EEG signal was recorded using an OpenBCI® EEG Electrode Cap kit (21 electrodes). The EEG data were collected at 250 Hz sampling frequency. Once acquired, EEG data were low-pass filtered at 40 Hz, high-pass filtered at 5 Hz and a 50 Hz Notch filter was also applied. Since the stimuli had to elicit VEP, electrodes located in the occipital and parietal regions [9], [14], [15] were chosen. Electrodes 'Ground', ' O1', 'O2', 'P3', 'P4', 'CPz', 'Cz', 'F3' and 'F4' whose locations correspond to the international 10-20 system (Fig. 1) were selected. EEG data were epoched into 3s windows according to the triggers of the onset of visual stimuli during the experimental task.

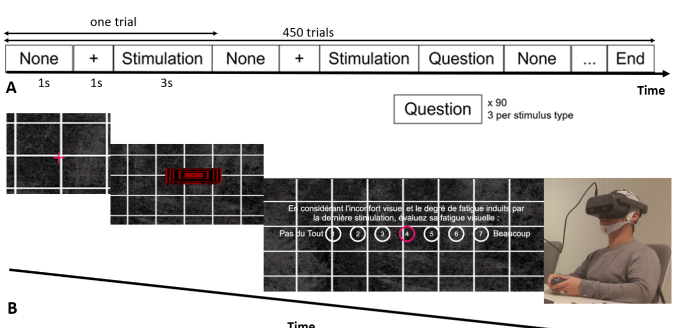

Fig. 1. **A**. Time sequence of the experiment/ **B**. Time sequence of a trial with the virtual environment (left to right) and the subject wearing the EEG cap, the HMD and carrying the controller while executing the task (right).

C. 3D Stimuli Inducing VEP

The visual 3D stimuli were generated using Unity's built-in Shader Graph tool [1]. The design of efficient VEP stimuli was inspired from the existing literature, and features to decrease visual fatigue were considered.

The targets consisted of a cuboid that behaved differently according to the stimulus types. The targets' positions were randomly changed so the participants would not lose motivation. For the duration of the task, targets were equiprobably located: up-right, bottom-right, bottom-left, and up-left on the scene. The frequency that modulated the stimuli aspect was set to 8 Hz to avoid epileptogenic frequencies – which is one major limitation of VEP-based BCI and limits visual comfort [6], [10], [15]. The color of the cuboid was set to red as this color was shown to be less uncomfortable for VEP stimuli in the low-frequency range [10]. The color amplitude was reduced to 60% as studies showed that lower contrasts or stimulation amplitude depth improved flickers ergonomics by reducing visual fatigue [16]. The virtual environment consisted of a dark cubic room with a grey grid pattern. The questions displayed on the wall in front of the participant and the targets (the cuboids with modulated behavior) appeared in the in-between space. Before each stimulation, a red cross cued the localization of the upcoming target (see Figure 1).

The 30 types of stimulations were split into two pattern categories: full (the whole cuboid was visible – i.e., the entire cuboid flickered) or fragmented (only 30 circular areas per face of the cuboid were visible – i.e., only parts of the cuboid flickered). The standard efficient VEP stimuli types and the c-VEP stimuli considered were the following: standard flash flicker (luminance variation of the object from black to full luminosity according to a sinusoidal modulation) [3], Newton's ring inspired flicker (concentric square ring with expanding movement) [25], grow-shrink stimulus [7] (an object whose size periodically changes from 60% up to 120% of its original size according to a sinusoidal function), a spinning motion around the vertical axis (according to a sine function) [12], [21] and a c-VEP flash flicker whose variation was controlled by a pseudo-random sequence square signal (further referred to as m-sequence) [3], [11], [20]. Combinations of these five basic stimuli defined the other stimulation types: all possible combinations of two sinusoidal variation-based stimulation types and the combination of the c-VEP flash with one sinusoidal-f-VEP stimulus. A video showing all the stimuli is presented here [22].

D. Experimental Design

Participants were instructed to stare at a target stimulus for 3 s per trial, with an inter-trial interval of 1s. Before each trial, a cross cue appeared at the location of the next target to indicate to the participant where to direct their gaze (see Figure 1 B). Once ready, they had to press the trigger of the right controller for 1 s. Each stimulus type randomly appeared 15 times; to assess the usability of each stimulation paradigm, participants had to answer a question at the end of the stimulation for 20% of the trials for each stimulus – three assessments per

 ISBN: 978-1-61208-995-9

type in total randomly distributed across the experiment (see Figure 1 A). The order of question occurrence was balanced according to the Latin square so that with 30 participants, we could reduce the order-effect when rating the fatigue level of one stimulation. Participants rated the visual fatigue level of each stimulus using the right controller: the joystick to select the score and then the trigger for 2 s to confirm their choice. Participants were instructed not to move or blink during the visual stimulation. The task had a minimum duration of 38 minutes – with no imposed breaks, and participants could control the resting time between each trial (trials started only if the trigger was pressed for 1 s).

E. EEG Data Analysis

Canonical Correlation Analysis (CCA) is often used when studying VEP-based BCI [18] to perform the automatic classification of VEP. However, this method is quite sensitive to inter-subject variability and the quality of the EEG recordings. Thus, EEGnet proposed by Lawhern et al. [17] to classify EEG signals has been adapted to classify VEP. Thirty classes corresponding to the thirty stimulation types were considered. Data were epoched and augmented so that 438 temporal windows could be given to each class. The EEGNet was trained for each subject (within-subject). Participants were asked to rate the fatigue level of each stimulation type three times during the task to evaluate flickers' ergonomics. The questionnaire was inspired by the visual analog scale [13], which is often used in clinical research to evaluate pain intensity; it is also used to rate the discomfort or fatigue of tasks. The question was written in French and could be translated as: "considering the visual discomfort and amount of tiredness induced by the last stimulation, rate its visual fatigue level." Participants could rate the stimulation from 1 to 7 (1: not tiring at all, 7: highest fatigue level) [5], [7].

III. Results

A. Offline Classification

The average offline recognition accuracy of the 30 classes corresponding to the different stimulation types was close to ceiling (M=97.58%, SD=.0.0066) across subjects, indicating that the EEGNet classifier was very effective at classifying stimuli of the same frequency that only difered via their visual characteristics (see Figure 2). Hence, the sole modification of the visual transformation of one target might be sufficient to modulate the induced EEG response and enable proper identification of the stimulation type. In addition, the accuracy results showed a weak inter-subject variability.

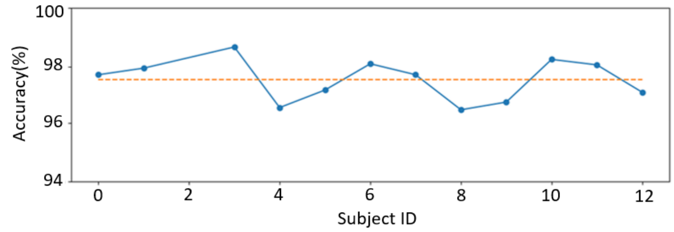

Fig. 2. Classification accuracies of EEGNet model over 30 classes corresponding to the 30 stimulation types for 11 participants. Accuracies ranged above 97%. Dotted orange line indicates the mean accuracy (M=97.58%, SD=.0.0066).

B. Stimuli Ergonomics

The analysis is conducted using Python. Since the data were not normally distributed using the Shapiro-Wilk test, a two-way repeated-measures Friedman ANOVA was performed to investigate the stimulation type's main effect on fatigue level score. The significant level was set to 0.05. A significant difference in the main effect was observed ($F = 95.31, DL = 10, p < 0.0001$). Thus, the type of stimulation could affect the scoring of its fatigue level, that is, its ergonomics. Wilcoxon signed-rank test was applied for each pair of the conditions to investigate the interaction effects of ergonomics and stimulation type. The False Discovery Rate (FDR) was corrected for the within-group comparison using the Benjamini-Hochberg procedure. The difference in the ergonomics rating for different stimuli could not be highlighted, so we could not conclude about the influence of the type of stimulation on the fatigue score. However, most of the participants rated the fatigue level of the different stimulus types in the range of 2.5 – 5 (See Figure 3 A). The combination of the c-VEP flash with a sine-modulated spinning motion in a fragmented pattern (highlighted in red in Figure 3A) was the only stimulation to have a mean fatigue level higher than 5. 12 stimuli had a mean average fatigue level per participant less than 4, i.e., were rated in the comfortable / no particular fatigue induced range (highlighted in green in Figure 3A). The sinusoidal modulation combining Newton's square range type and grow-shrink motion (28 on Figure 3A) had the lowest standard deviation, suggesting a good overall appreciation from participants. Interestingly, the hybrid c-VEP and f-VEP flash with both full and fragmented patterns were part of stimuli with an acceptable fatigue level. These results are consistent with the pattern's effect when considering the standard deviation values.

Wilcoxon signed-rank test was used to explore the possible role of the completeness effect (full vs. fragmented pattern). The average answers per subject for all stimulation types of patterns 'full' to those of pattern 'fragmented' were significantly different ($Z = 1777, p < 0.0001$). Thus, the type of completeness could affect the scoring of the fatigue level of the stimulation, with full pattern stimuli possibly being less disturbing or less uncomfortable than fragmented stimulations (see Figure 3). Indeed, the average fatigue score in the fragmented condition was higher than that in the full condition (M=4.58, SD=1.39 vs.M= 3.65, SD=0.98).

IV. Conclusion and Future Work

In order to find ergonomic visual stimulations to be implemented in a future VEP-based BCI-VR, efficient 2D VEP stimuli were converted into 3D VEP stimuli within a virtual environment. The EEGNet model managed to classify the different stimuli with a high level of accuracy based on their

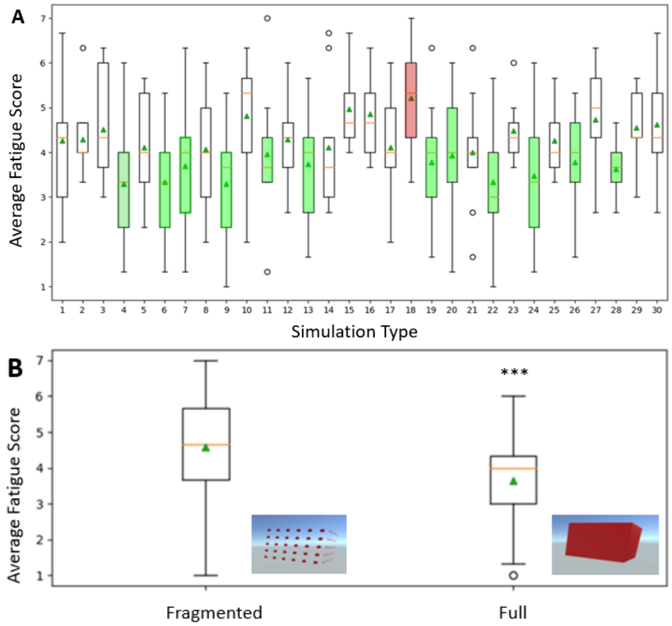

Fig. 3. **A**. Average fatigue score per stimulation type, n=11 participants, (flicker inducing most fatigue highlighted in red and flickers inducing the least fatigue highlighted in green in A Figure 3) **B**. Average fatigue score depending on the pattern, n=11 participants

visual differences, which suggested that the different types of stimulation did induce VEP with their very own specific EEG signatures. This pilot study paves the way for immersive BCI-VR research and applications using 3D targets.

However due to the small number of participants, the EEG-net classification and ergonomic analyses should be nuanced but they give a good idea of the trends. More participants should be included in the study to improve the statistical power. Moreover, the EEG recording system consisted of a consumer kit with a sampling frequency of only 250hz. This could be a limitation for the accuracy of the EEG signals but as the study was intended to be applied directly to an industrial project, using the OpenBCI EEG cap kit for such a study was part of the contributions – as for the VR headset used.

In order to lighten the experimental task, we used a subjective method for assessing visual fatigue, based on a simple question [5], [7]. However, more comprehensive questionnaires could improve the accuracy of the ergonomics score in future works and the analysis of brain rythms could provide an objective evaluation method of induced fatigue (depending on the stimuli presentation and their occurence in the task) while taking advantage of the EEG recording [4].

Finally, the next step will be integrating these ergonomics flickers into a VR-based BCI application to help future patients' rehabilitation. As for existing studies in the literature, eye movements were not monitored. Using a VR headset allowing eye tracking could control this parameter and avoid artifacts in the EEG signal.

References

[1] Unity real-time development platform | 3d, 2d VR & AR engine.

[2] R. Abiri, S. Borhani, E. W. Sellers, Y. Jiang, and X. Zhao. A comprehensive review of eeg-based brain–computer interface paradigms. *Journal of neural engineering*, 16(1):011001, 2019.

[3] G. Bin, X. Gao, Y. Wang, B. Hong, and S. Gao. Vep-based brain-computer interfaces: time, frequency, and code modulations [research frontier]. *IEEE Computational Intelligence Magazine*, 4(4):22–26, 11 2009.

[4] T. Cao, F. Wan, C. M. Wong, J. N. da Cruz, and Y. Hu. Objective evaluation of fatigue by eeg spectral analysis in steady-state visual evoked potential-based brain-computer interfaces. *Biomedical Engineering Online*, 13(1):28, 3 2014. PMID: 24621009 PMCID: PMC3995691.

[5] X. Chai, Z. Zhang, K. Guan, T. Zhang, J. Xu, and H. Niu. Effects of fatigue on steady state motion visual evoked potentials: Optimised stimulus parameters for a zoom motion-based brain-computer interface. *Computer Methods and Programs in Biomedicine*, 196:105650, 11 2020.

[6] X. Chen, Y. Wang, S. Zhang, S. Xu, and X. Gao. Effects of stimulation frequency and stimulation waveform on steady-state visual evoked potentials using a computer monitor. *Journal of Neural Engineering*, 16(6):066007, 10 2019. PMID: 31220820.

[7] K.-M. Choi, S. Park, and C.-H. Im. Comparison of visual stimuli for steady-state visual evoked potential-based brain-computer interfaces in virtual reality environment in terms of classification accuracy and visual comfort. *Computational Intelligence and Neuroscience*, 2019:9680697, 2019. PMID: 31354804 PMCID: PMC6636533.

[8] A. Craig, Y. Tran, N. Wijesuriya, and P. Boord. A controlled investigation into the psychological determinants of fatigue. *Biological psychology*, 72(1):78–87, 2006.

[9] A. M. Dreyer and C. S. Herrmann. Frequency-modulated steady-state visual evoked potentials: A new stimulation method for brain–computer interfaces. *Journal of Neuroscience Methods*, 241:1–9, 2 2015.

[10] X. Duart, E. Quiles, F. Suay, N. Chio, E. García, and F. Morant. Evaluating the effect of stimuli color and frequency on ssvep. *Sensors (Basel, Switzerland)*, 21(1):117, 12 2020. PMID: 33375441 PMCID: PMC7796402.

[11] S. et al. Introducing chaotic codes for the modulation of code modulated visual evoked potentials (c-vep) in normal adults for visual fatigue reduction. *PLoS ONE*, 14(3):e0213197, 3 2019. PMID: 30840671 PMCID: PMC6402685.

[12] W. et al. Steady-state motion visual evoked potential (ssmvep) based on equal luminance colored enhancement. *PLoS ONE*, 12(1):e0169642, 1 2017. PMID: 28060906 PMCID: PMC5218567.

[13] M. Hayes. Experimental developement of the graphics rating method. *Physiol Bull*, 18:98–99, 1921.

[14] S. P. Heinrich. A primer on motion visual evoked potentials. *Documenta Ophthalmologica. Advances in Ophthalmology*, 114(2):83–105, 3 2007. PMID: 17431818.

[15] C. S. Herrmann. Human eeg responses to 1-100 hz flicker: resonance phenomena in visual cortex and their potential correlation to cognitive phenomena. *Experimental Brain Research*, 137(3-4):346–353, 4 2001. PMID: 11355381.

[16] S. Ladouce, L. Darmet, J. Torre Tresols, G. Ferraro, and F. Dehais. Improving user experience of ssvep-bci through reduction of stimuli amplitude depth. pages 2936–2941, 2022.

[17] V. J. Lawhern, A. J. Solon, N. R. Waytowich, S. M. Gordon, C. P. Hung, and B. J. Lance. Eegnet: A compact convolutional network for eeg-based brain-computer interfaces. *Journal of Neural Engineering*, 15(5):056013, 10 2018. arXiv:1611.08024 [cs, q-bio, stat].

[18] F. Lotte, L. Bougrain, A. Cichocki, M. Clerc, M. Congedo, A. Rakotomamonjy, and F. Yger. A review of classification algorithms for eeg-based brain–computer interfaces: a 10 year update. *Journal of Neural Engineering*, 15(3):031005, 4 2018. publisher: IOP Publishing.

[19] P. Martinez, H. Bakardjian, and A. Cichocki. Fully online multicommand brain-computer interface with visual neurofeedback using ssvep paradigm. *Computational intelligence and neuroscience*, 2007, 2007.

[20] V. Martínez-Cagigal, J. Thielen, E. Santamaría-Vázquez, S. Pérez-Velasco, P. Desain, and R. Hornero. Brain–computer interfaces based on code-modulated visual evoked potentials (c-VEP): a literature review. *Journal of Neural Engineering*, 18(6):061002, nov 2021.

[21] M. Rekrut, T. Jungbluth, J. Alexandersson, and A. Krüger. Spinning icons: Introducing a novel ssvep-bci paradigm based on rotation. In *26th International Conference on Intelligent User Interfaces*, IUI '21, page 234–243, New York, NY, USA, 2021. Association for Computing Machinery.

 ISBN: 978-1-61208-995-9

[22] Thibault Porssut. Ergonomic 3d flickers for VEP-based BCI paradigm to interact in virtual reality using deep learning.

[23] N. R. Waytowich, Y. Yamani, and D. J. Krusienski. Optimization of checkerboard spatial frequencies for steady-state visual evoked potential brain-computer interfaces. *IEEE transactions on neural systems and rehabilitation engineering: a publication of the IEEE Engineering in Medicine and Biology Society*, 25(6):557–565, 6 2017. PMID: 27542113.

[24] J. R. Wolpaw, N. Birbaumer, D. J. McFarland, G. Pfurtscheller, and T. M. Vaughan. Brain–computer interfaces for communication and control. *Clinical Neurophysiology*, 113(6):767–791, 2002.

[25] J. Xie, G. Xu, J. Wang, F. Zhang, and Y. Zhang. Steady-state motion visual evoked potentials produced by oscillating newton's rings: implications for brain-computer interfaces. *Plos one*, 7(6):e39707, 2012.

[26] D. Zhu, J. Bieger, G. Garcia Molina, and R. M. Aarts. A survey of stimulation methods used in ssvep-based bcis. *Computational intelligence and neuroscience*, 2010.